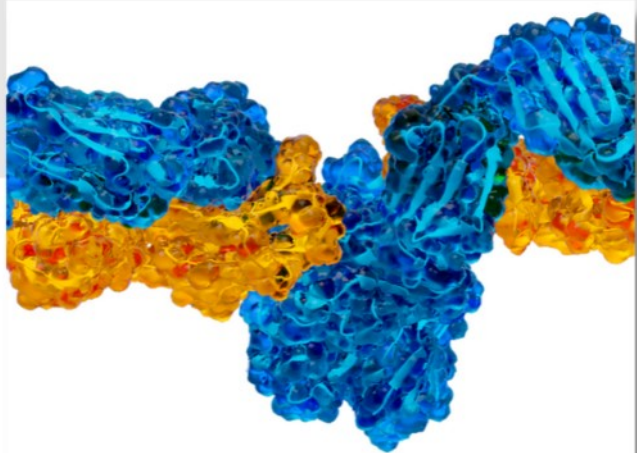




Harnessing iCIEF to Unlock Protein-Based Therapeutics



Harnessing iCIEF to Unlock Protein-Based Therapeutics

ARTICLE COLLECTION

WILEY Analytical Science

Sponsored by:
biotechne protein simple

Read the new Article Collection

Keep up to date with the latest developments in biotherapeutics and the range of treatments for various diseases with our latest article collection. Find out how imaged CIEF (iCIEF) technique is essential for quality control and analytical development of these drugs, as it accurately determines the surface charge of lipid nanoparticles and the charge heterogeneity of proteins and antibodies.

This article collection aims to provide you with more information on these techniques and technologies, helping you further your research in this field.

biotechne protein simple

WILEY

Stimuli-Responsive 3D Printable Conductive Hydrogel: A Step toward Regulating Macrophage Polarization and Wound Healing

Jieun Lee, Sayan Deb Dutta, Rumi Acharya, Hyeonseo Park, Hojin Kim, Ayushi Randhawa, Tejal V. Patil, Keya Ganguly, Rachmi Luthfikasari, and Ki-Taek Lim*

Conductive hydrogels (CHs) are promising alternatives for electrical stimulation of cells and tissues in biomedical engineering. Wound healing and immunomodulation are complex processes that involve multiple cell types and signaling pathways. 3D printable conductive hydrogels have emerged as an innovative approach to promote wound healing and modulate immune responses. CHs can facilitate electrical and mechanical stimuli, which can be beneficial for altering cellular metabolism and enhancing the efficiency of the delivery of therapeutic molecules. This review summarizes the recent advances in 3D printable conductive hydrogels for wound healing and their effect on macrophage polarization. This report also discusses the properties of various conductive materials that can be used to fabricate hydrogels to stimulate immune responses. Furthermore, this review highlights the challenges and limitations of using 3D printable CHs for future material discovery. Overall, 3D printable conductive hydrogels hold excellent potential for accelerating wound healing and immune responses, which can lead to the development of new therapeutic strategies for skin and immune-related diseases.

1. Introduction

The process of wound healing is intricate and constantly changes to repair and restore the structure and function of injured tissues. Traditional wound-healing approaches have limitations in

J. Lee, S. D. Dutta, R. Acharya, H. Park, H. Kim, A. Randhawa, T. V. Patil, K. Ganguly, R. Luthfikasari, K.-T. Lim

Department of Biosystems Engineering
Kangwon National University
Chuncheon 24341, Republic of Korea
E-mail: ktlim@kangwon.ac.kr

J. Lee, R. Acharya, H. Park, H. Kim, A. Randhawa, T. V. Patil, K.-T. Lim
Interdisciplinary Program in Smart Agriculture
Kangwon National University
Chuncheon 24341, Republic of Korea

S. D. Dutta, K.-T. Lim
Institute of Forest Science
Kangwon National University
Chuncheon 24341, Republic of Korea

 The ORCID identification number(s) for the author(s) of this article can be found under <https://doi.org/10.1002/adhm.202302394>

DOI: 10.1002/adhm.202302394

addressing the various efficacies and aspects of wound repair. One of the main drawbacks is the pain caused during removal of dressings owing to attachment to newly grown granulations.^[1] In addition, they exhibit low oxygen permeability, lack biomimetic properties, and have difficulty achieving optimal drug loading levels. Therefore, innovative approaches are needed to accelerate wound healing and promote tissue regeneration. In recent years, the development of 3D printable conductive hydrogels has garnered significant interest for wound-healing applications.^[2] These hydrogels combine the unique properties of conductivity and the versatility of 3D printing technology, enabling the fabrication of customized scaffolds with precise geometric shapes and controlled structures.^[3]

Hydrogels are used for various medical purposes because of their flexibility and biocompatibility. Using 3D printing technology, these hydrogels can be manufactured into materials with intricate structures. It is anticipated that 3D-printed hydrogels will promote skin regeneration and aid wound healing when applied to wound sites.^[4] These conductive hydrogels exhibit excellent biocompatibility, biodegradability, and mechanical properties suitable for wound healing.^[5] They create a moist environment at the wound site, facilitate cell migration and proliferation, prevent excessive scar formation, and maintain a favorable microenvironment for tissue regeneration.^[6]

Furthermore, conductive hydrogels comprise a water-soluble polymer network infused with conductive materials, such as carbon nanotubes (CNTs), graphene, or conductive polymers.^[7] These materials impart electrical conductivity to the hydrogel, enabling the electrical stimulation (ES) of the wound site. Electrical stimulation has been proven to promote cell migration, proliferation, and differentiation; enhance angiogenesis; and regulate inflammatory responses, thereby accelerating wound healing.^[8] In addition, conductive hydrogels can serve as versatile platforms for the localized delivery of bioactive molecules, including growth factors, cytokines, and therapeutic drugs.^[2a,9] By incorporating these bioactive substances into the hydrogel matrix, sustained and controlled release can be achieved, providing a spatiotemporal delivery system that mimics the dynamic nature of the

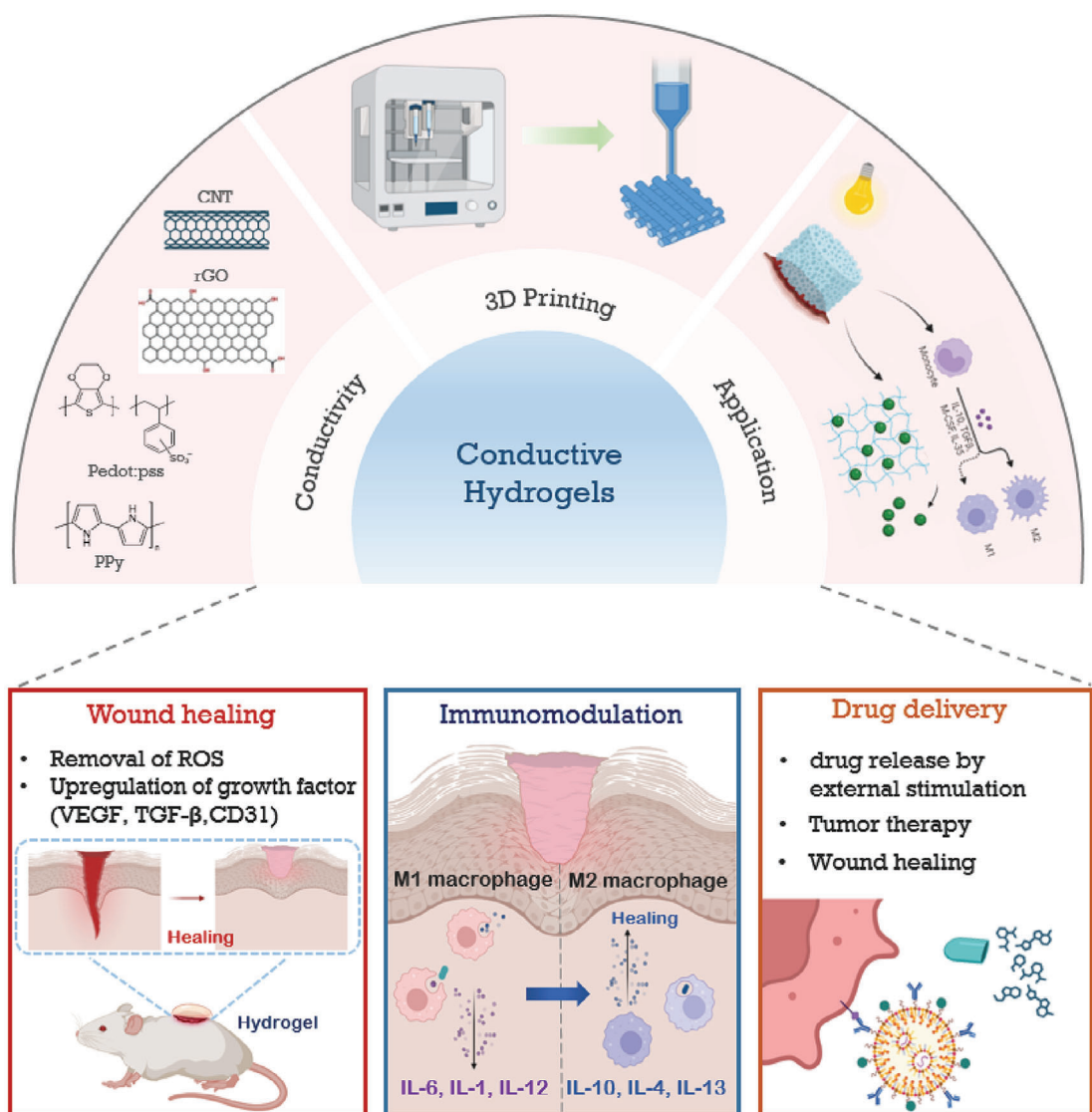


Figure 1. The overall schematic diagram of electrical conductivity material-based 3D printing applications.

wound-healing process. These capabilities open new avenues for targeted therapies and personalized medical approaches for wound healing. These materials are also vital for modulating the immune response during wound healing.^[10] Excessive or prolonged inflammatory responses pose significant challenges to tissue regeneration during wound healing. Therefore, integrating immunomodulatory capabilities into conductive hydrogels can improve overall healing outcomes by creating a balanced inflammatory environment.^[11]

Despite significant advancements in 3D printable conductive hydrogels for wound healing, some challenges still need to be addressed. These involve optimizing hydrogel properties, such as mechanical strength, to meet the specific requirements of various wound types, biocompatibility of scaffold materials, and degradation rates.^[5a,12] In addition, the precise control of electrical stimulation parameters and the integration of suitable bioactive molecules add further complexity. Moreover, transitioning these innovative hydrogel systems from the laboratory to clinical set-

tings requires comprehensive translational research and regulatory considerations.

This review presents a comprehensive overview of the latest advancements in 3D printable conductive hydrogels for wound healing and immunomodulation. Herein, we discuss the fabrication techniques, physicochemical properties, and biological functionalities of these hydrogels. Furthermore, we highlight the challenges and future directions in this exciting field, aiming to accelerate the development and clinical application of 3D printable conductive hydrogels for improved wound-healing outcomes (Figure 1).

2. Conductive Materials in Tissue Engineering

Conductive polymers (CPs) are organic materials with electrical conductivity and optical properties similar to those of inorganic semiconductors and metals.^[13] CPs can be synthesized in various types using diverse, simple, and cost-effective methods.^[14]

Table 1. Major components of conductive hydrogels for wound-healing application.

Classification of CHs	Components of the polymer network	Conductive biopolymer	Conductivity [S m^{-1}]	Electrical stimuli	Tensile stress	Application	Ref.
Conductive polymers only	PPy-PAAm	PPy	0.3	0–900 mV	136.3 MPa	Wearable electronic devices, electro- stimulated drug-release systems	[18]
	PAM/SHA/PANI	PANI	0.105–0.12	DC, 3 V, 0.1–100 Hz	13 kPa	Infected chronic wound healing	[19]
	PEDOT/PSS/GG/HA	PEDOT:PSS	0.127	0.8 V	0.3 MPa	Supercapacitors, all-in-one wound dressing	[20]
Metal-based conductive polymer hydrogels	OSA/CMCS/AgNPs	AgNPs	0.127	DC, 100 mV, 1 Hz	10 kPa	Self-healing, wound dressings	[21]
	PDA/PAM	Au@PDA	6×10^{-6}	N/A	53 kPa	Biosensors, electric skins, health monitoring	[22]
Carbon-based conductive polymer hydrogels	Ag@Cu	Cu	1.35×10^{-2}	N/A	1.5 MPa	Wound dressing	[23]
	CNT/Gel/CS/PDA	CNTs	0.062–0.072	N/A	115.9 kPa	Biomedical engineering, electrical devices	[24]
	GO/Cellulose	GO	>6	≈ 300 mV, 10^2 – 10^5 Hz	130 kPa	E-skin	[25]
	HA-DA	rGO	0.005	N/A	65.1 kPa	Wound-healing dressings	[26]
	MXene/Cellulose	MXene	2.83×10^{-3} to 7.04×10^{-2}	100 V mm^{-1}	N/A	Wound-healing dressings	[27]

PPy: polypyrrole, PANI: polyaniline, AgNPs: silver nanoparticles, PDA: polydopamine; PAM: polyacrylamide, CNTs: carbon nanotubes, AuNPs: gold nanoparticles, GO: graphene oxide, rGO: reduced graphene oxide.

The conductivity of CPs arises from the delocalized π -electrons along the polymer chains, facilitating charge transport.^[15] However, manufacturing conductive wound-dressing hydrogels using pure CPs is challenging because of their poor mechanical and solubility characteristics and processability.^[13] Conductive polymer hydrogels (CPHs) are polymer materials that combine conductive polymers with hydrogels to provide electrical conductivity and flexibility.^[16] In addition, CPHs provide excellent interfaces between systems, such as electrodes, electrolytes, and biological and synthetic systems, making them highly promising for various applications, including electrode materials for energy storage devices, biofuel cells, and biomedical applications^[17] (Table 1).

2.1. Conductive Polymers

Polyacetylene (PA), polyaniline (PANI), polythiophene (PT), polypyrrole (PPy), and poly(3,4-ethylenedioxythiophene):poly(styrene sulfonate) (PEDOT:PSS) are widely known CPHs^[4] that have been extensively studied for wound healing because of their excellent electrical properties.

2.1.1. Polypyrrole

PPy is considered one of the most promising materials in biomedicine because of its convenient synthesis, suitable biocompatibility, low cost, surface modification versatility, excellent environmental resistance, and high electrical conductivity.^[28] In biomedical applications, PPy is electrochemically generated by integrating anionic species such as proteins and polysaccharides, which carry negative charges, to form composite materials.^[29]

Figure 2A shows the chemical structures of PPy before and after doping. PPy is highly rigid, insoluble, and has poor processability owing to its high degree of crosslinking with the molecular back-

bone. Therefore, the use of PPy as a standalone material is challenging and must be optimized in a mechanically manageable or processable form.^[28b] By mixing PPy with other biocompatible and biodegradable polymers such as poly(acrylic acid) (PAA), chitosan (CS), poly-L-lactide (PLLA), and alginate (Alg), its properties can be adjusted, expanding its potential applications as a biomaterial for bioelectronic devices.^[30] Sajesh et al. mixed PPy with alginate to improve cell interactions and evaluated its potential for skeletal tissue engineering by incorporating chitosan to obtain mechanically stable scaffolds. They confirmed the biocompatibility of the developed scaffold and demonstrated that chitosan/PPy-Alg composite scaffolds could serve as substrates for tissue regeneration.^[31] Electric field (EF) has a promising effect on wound healing. However, it alone cannot stimulate the entire wound area. Wang et al. developed an electrically active hydrogel based on bacterial cellulose (rBC).^[32] A hydrogel produced by mixing CNTs and PPy NPs (≈ 100 nm) to impart electrical conductivity exhibited excellent thermal stability, mechanical properties, resilience, and moisture absorption capacity. In particular, the addition of PPy and CNTs increased the conductivity of the rBC/PPy/CNT hydrogel by up to 10^7 times compared with that of the rBC hydrogel. Electrical stimulation of the wound area can enhance the healing process or regulate the release rate of the therapeutics. Furthermore, in vitro studies on fibroblast cells (NIH3T3 cells) showed better cell spreading and higher cell proliferation (18% higher after 3 d) in the PPy/Alg hydrogel than in pure rBC. Fibroblast proliferation and migration play crucial roles in wound healing and can be further enhanced by increasing the intracellular Ca^{2+} concentration through EF stimulation.^[33]

2.1.2. Polyaniline

PANI is a polymer whose conjugative π -bond structure allows the mobility of electrons on its chain, rendering it electrically

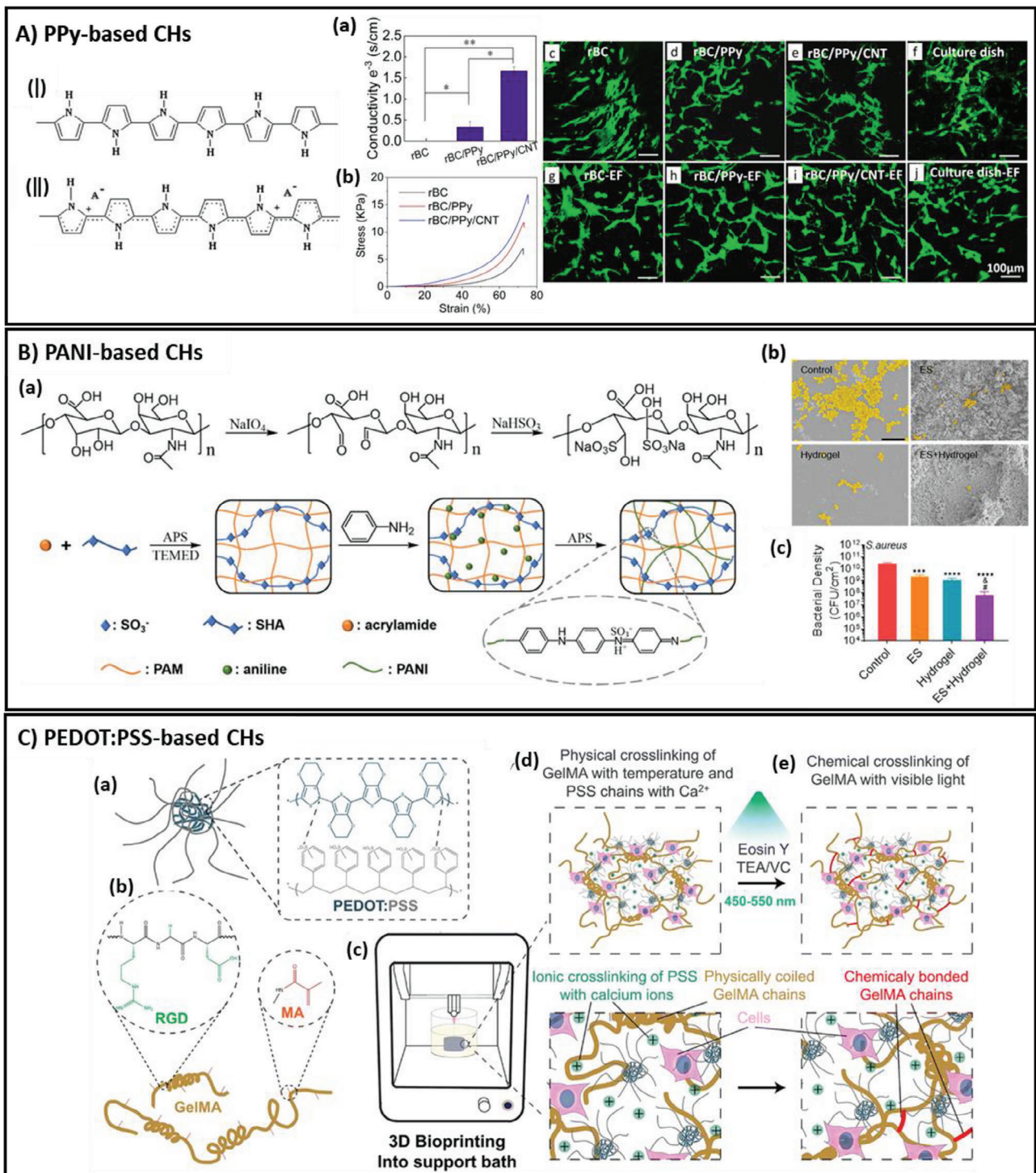


Figure 2. Conductive-polymer-based CHs. A) PPy-based CHs. Chemical structure of PPy: (I) before doping and (II) after doping. Reproduced with permission.^[28b] Copyright 2011, Wiley-VCH GmbH. a) Hydrogels with BC, rBC, rBC/PPy, and rBC/PPy/CNT electrical conductivity. b) rBC, rBC/PPy, and rBC/PPy/CNT hydrogel's compressive stress-strain curves. NIH3T3 cells were cultivated on hydrogels and in culture dishes for 3 d, c-f) without EF and g-j) with EF. Live/dead labeling of the cells is shown in (c)-(f). Here, the rBC, rBC/PPy hydrogels, rBC/PPy/CNTs hydrogel, and culture dish are represented by (c) and (g), (d) and (h), (e) and (i), (f) and (j), respectively. Reproduced with permission.^[32] Copyright 2020, Elsevier. B) CHs based on PANI. a) Preparation of the PSP hydrogel. Evaluation of in vivo wound healing: b) SEM image (with the scale bar of 5 μ m) of *S. aureus* from diverse groups after incubation in TSB. c) Surface density of attached bacteria in another group. *P*-values of 0.05, 0.01, 0.001, and 0.0001 are indicated by the *, **, ***, and ****, respectively. Statistically significant differences ($n = 3$) from the control, ES, and hydrogel groups are shown by the symbols *, &, #, respectively. Reproduced with permission.^[19] Copyright 2021, American Chemical Society. C) Creating conductive GelMA/PEDOT:PSS bioinks to create constructions with cells. Reproduced with permission.^[39] Copyright 2019, American Chemical Society.

conducting.^[34] Among the many conductive polymer materials, PANI stands out for its simplicity of processing, easy integration with other hydrogel materials, and desirable properties such as water solubility, low toxicity, excellent environmental stability, and nanostructured morphology.^[35] It also exhibits excellent biocompatibility and conductivity, making it suitable for various biomedical applications. However, they also have unfavorable properties such as low processability, insolubility, poor solubility, and low degradability. A wound-healing dressing was developed to address these limitations by adjusting its mechanical properties, electrical conductivity, and processability. Wu et al. developed a PANI-based hydrogel with antimicrobial, conductive, and flexible properties for the treatment of chronic wounds^[19] (Figure 2B). PANI was incorporated into a polyacrylamide (PAM) matrix hydrogel by *in situ* polymerization of preabsorbed aniline molecules to obtain a PANI hydrogel. The improved mechanical properties were attributed to the robust structure of PANI and the dynamic hydrogen bonds formed between the PANI chains and between PANI and PAM, which enabled efficient energy dissipation. Recently, supramolecular polymeric hydrogels combining polymers with low-molecular-weight gelators (LMWG) have been developed. Researchers demonstrated that hemostatic, antioxidant, antibacterial, and drug-free H/G4-HA(Cu)/PANI accelerated the wound-healing process by promoting wound closure, collagen deposition, and the upregulation of CD31 expression, as evidenced by a full-thickness skin defect model in mice.^[36] These findings highlight the potential of hydrogels incorporating PANI as promising wound dressing materials.

2.1.3. Poly(3,4-ethylenedioxythiophene):Poly(styrene sulfonate)

PEDOT:PSS is the most well-known conducting polymer electrolyte composite, and is a highly doped p-type semiconductor. The sulfonate anions balance the voids or vacancies in the positively charged PEDOT chains on the negatively charged PSS chains, which serve as counterions.^[37] Incorporating PEDOT:PSS enhances the interaction between the two materials, improving their mechanical strength and expansibility and reducing hydrophobicity.^[8a] Furthermore, PEDOT:PSS is an ideal material for manufacturing 3D printable conductive hydrogels because of its excellent chemical stability, high conductivity, biocompatibility, and superior film-forming properties.^[8a,38] For instance, gelatin methacryloyl (GelMA) and PEDOT:PSS were synthesized and utilized in bioprinting to form 3D cell-laden structures (Figure 2C). In addition to the photo-crosslinking of GelMA, PEDOT:PSS can form secondary crosslinks with Ca^{2+} under visible light, enhancing the network. The conductivity-based bioinks and printing methods presented herein have the potential to fabricate complex, cell-laden, and electrically active structures. These structures can be helpful in applications involving cell transplantation for the regeneration of electrically active tissues.^[39] Fibroblast growth and movement are vital for wound healing and these mechanisms can be further augmented by electrical stimulation. In conclusion, although conducting polymers based on conjugated polymers have seen significant advancements, uneven dispersion, monomer toxicity, and other issues continue to hinder their development.

2.2. Metal Nanoparticles

Recently, the introduction of various nanoparticles for wound healing has led to remarkable advancements in wound treatments. Antimicrobial nanoparticles, such as silver nanoparticles (AgNPs), gold nanoparticles (AuNPs), and copper nanoparticles (CuNPs), have shown low cytotoxicity, antibacterial properties, and biocompatibility, accelerating the wound-healing process.^[40] Due to their large surface area, these nanoscale metallic materials can be easily modified chemically or physically and exhibit excellent biocompatibility and conductivity.^[13]

2.2.1. Silver Nanoparticles

AgNPs possess excellent antimicrobial, antifungal, anti-inflammatory, and wound-healing properties, making them highly effective in various wound dressings.^[41] The antimicrobial actions of these particles can be categorized into two types: inhibitory and bactericidal. The AgNPs exhibited low toxicity, did not cause skin discoloration, and were effective at low concentrations.^[42] This mechanism involves the generation of reactive oxygen species (ROS) resulting from the inhibition of respiratory enzymes by Ag^+ ions, leading to cell death. Bacterial cells contain sulfur and phosphorus, which act as soft bases and interact with the AgNPs as soft acids, thereby triggering apoptosis.^[40] For instance, Wu et al. produced nanostructured AgNP-BC by self-assembling nanoparticles formed on the surface of nanofibers derived from bacterial cellulose (BC). In biomedical research, AgNP-BC hydrogel membranes have been shown to effectively reduce bacterial proliferation on wound surfaces and promote wound healing.^[43] In another study, Palem et al. developed nanocomposite (AgNC) hydrogel with injectable and bacterial inactivation properties.^[44] A fast-forming AgNC hydrogel was produced by distal addition of a guar gum-grafted polyacrylamide glycolic acid (GG-g-PAGA) polymer, silver nitric acid (AgNO_3), and sodium borohydride (NaBH_4) (Figure 3A). The hydrophilic surface of AgNCs effectively delayed the evaporation of moisture inside the wound and provided a long-term moist wound environment. In addition, the swelling of the hydrogel is directly related to its porosity, and the inclusion of AgNPs can increase the porosity of the nanocomposites, facilitate the absorption of emissions from wounds, and promote cell proliferation. The PAGA@AgNC hydrogel exhibited self-healing ability, injectability, elasticity, fluidity, high swelling, porosity, upright mechanical behavior, and biodegradability. However, in addition to the toxicity of silver and the potential thrombosis risk of nanoparticles, the *in situ* formation characteristics that confer the advantages of silver nanoparticles are accompanied by the introduction of toxic reducing agents during their preparation. These factors make the application of Ag indeterminate.^[15]

2.2.2. Gold Nanoparticles

AuNPs are the most commonly used metal in biomedicine. They possess various characteristics such as adjustable size, shape, surface properties, optical properties, biocompatibility, and high stability.^[15,45] AuNPs exhibit unique optical properties, such as

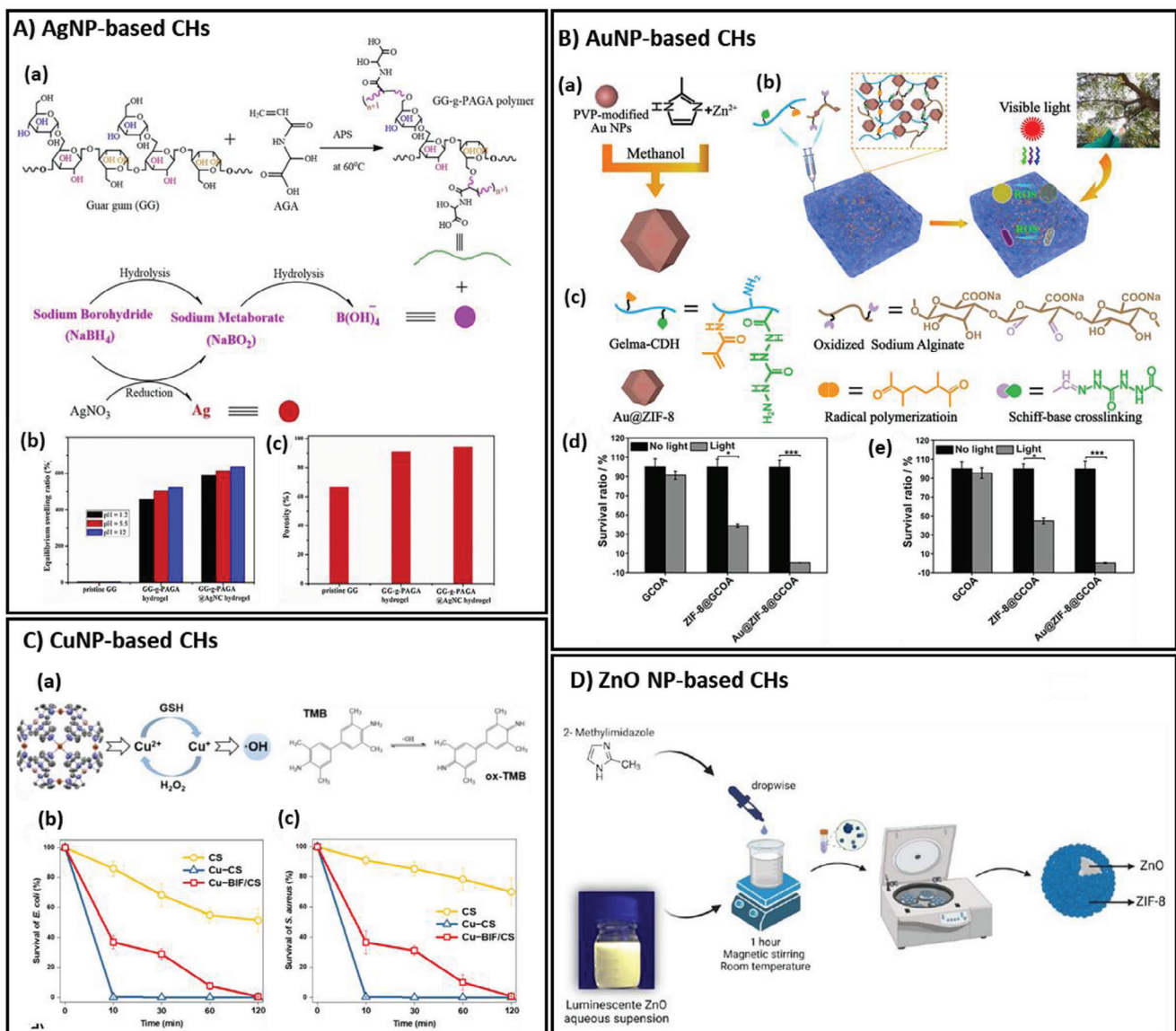


Figure 3. Metal nanocrystals-based CHs. A) AgNP-based CHs. a) Graphic representation of the GG-g-PAGA and GG-g-PAGA@AgNC hydrogel preparation mechanisms. b) A pH-based investigation of swelling. c) Analysis of the porosity of hydrogels made of pure GG, GG-g-PAGA, and GG-g-PAGA@AgNC. Reproduced with permission.^[44] Copyright 2019, Elsevier. B) AuNP-based CHs. a) Schematic illustration of the syntheses of Au@ZIF-8. b) Visual representation of Au@ZIF-8 incorporated into hydrogels for light-activated infection model treatment. On a Luria-Bertani agar plate, visible colony units of *S. aureus* are shown in (e). ** $P = 0.01$, *** $P = 0.001$. Reproduced with permission.^[48] Copyright 2021, Elsevier. C) a) Outline of Fenton-like reaction mechanism. The survival rates of b) *E. coli* and c) *S. aureus* were determined by the colony-forming unit (CFU) method after various treatments. Reproduced with permission.^[57] Copyright 2022, Elsevier. D) Schematic of ZnO@ZIF-8 NPs formation. Reproduced with permission.^[59] Copyright 2023, MDPI.

plasmon resonance.^[46] This phenomenon occurs when the electrons of gold respond to incoming radiation, causing resonance and resulting in the absorption and scattering of light. This effect can be utilized to either locally heat or destroy tissues, or to release therapeutic payload molecules. Furthermore, AuNPs can be used in therapeutic applications because they reduce the production of pro-inflammatory cytokines, including IL-6, IL-12, and TNF- α .^[47] However, similar to Ag, there is a potential risk of cellular toxicity during the preparation and in vivo delivery of AuNPs; thus, caution should be exercised. Recent reports have

indicated that injectable hydrogels prepared by encapsulating AuNPs within ZIF-8 can promote cellular growth^[48] (Figure 3B). The photocatalytic ROS generation properties of AuNPs under visible light enabled them to exhibit antimicrobial effects, locally inhibit bacterial growth, and accelerate wound healing. This injectable hydrogel system demonstrates excellent physical flexibility, elasticity, high biocompatibility, appropriate biodegradability, and superior antimicrobial efficacy. Recently, there has been considerable attention toward advancing effective and eco-friendly synthesis methods for metal nanoparticles in nanotechnology.

Hashem et al. synthesized a nanocomposite with antimicrobial activity using chitosan and AuNPs.^[49] Chitosan has been found to inhibit both gram-positive and gram-negative bacteria by disrupting their cell wall structures. Furthermore, an injectable AuNP hydrogel, prepared through gallic-tethering via NaIO_4 -induced crosslinking, exhibits high self-healing capability (up to 84.5%), injectability, tunable mechanical properties, flexible elasticity, and a macroporous structure. This was achieved through covalent and supramolecular interactions.^[50]

2.2.3. Copper Nanoparticles

Copper (Cu) plays a critical role in skin formation. It is essential for angiogenesis, synthesis, and stabilization of extracellular matrix (ECM) skin proteins.^[51] CuNPs possess excellent antimicrobial properties and can effectively promote wound healing by modulating various cytokine and growth factor signaling mechanisms, stimulating angiogenesis, and facilitating collagen deposition.^[52] CuNPs are gaining attention owing to their low cost, high stability, and potential for improved clinical safety.^[53] Moreover, CuNPs are inherently involved in all stages of wound healing.^[54] Effective wound dressings should stimulate rapid angiogenesis to supply oxygen and nutrients to cells at the wound sites.^[53] According to research, CuNPs have been shown to increase the expression of hypoxia-inducible factor-1 α (HIF-1 α) and regulate the secretion of vascular endothelial growth factor (VEGF), thereby promoting angiogenesis.^[55] However, the use of growth factors is typically associated with drawbacks, such as high cost, potential adverse effects when administered at supra-physiological doses, and loss of bioactivity.^[53] In another study, CuNPs induced the generation of ROS within bacterial cells, thereby inhibiting bacterial growth and division. These CuNPs exhibited excellent biocompatibility with HEK-293 and HeLa cell lines, while reducing cell-cell aggregation and matrix destabilization, promoting the remodeling of bacterial biofilms and membrane dissolution, and enhancing the efficacy of antibacterial agents.^[56] Wang et al. fabricated a chitosan membrane loaded with copper-bismuth-imidazole framework (Cu-BIF/CS) (Figure 3C) that maintained excellent cell compatibility, while releasing Cu^{2+} relatively slowly to kill bacteria. Importantly, the composite membrane demonstrated the potential to enhance wound healing and promote skin regeneration through the combined therapy of chitosan, Cu^{2+} , and hydroxyl radicals in infected wound-healing processes.^[57]

2.2.4. ZnO Nanoparticles

Recently, an increasing number of researchers have begun basic research on antibacterial activity because ZnO nanoparticles are stable under harsh processing conditions and are generally considered safe for humans and animals.^[58] The antimicrobial action of ZnO NPs can be explained by three main mechanisms: 1) generation of ROS, 2) release of Zn^{2+} ions, and 3) interactions between the NPs and the cell wall. These mechanisms promote the internalization of ZnO NPs into cells, causing damage to the cellular components. Another determinant of the antimicrobial efficacy of ZnO NPs is size. Smaller NPs have larger surface areas, increased interactions with bacterial cell constituents,

and enhanced antimicrobial activities. As shown in Figure 3D, even after the formation of ZIF-8, the ZnO nanoparticles maintained their luminescence. This result demonstrates that the size of the ZnO nanoparticles did not increase or increase only minimally. This is a highly significant finding, as it has been previously established that the size of nanoparticles influences their antibacterial activity, with smaller nanoparticles exhibiting better activity.^[59]

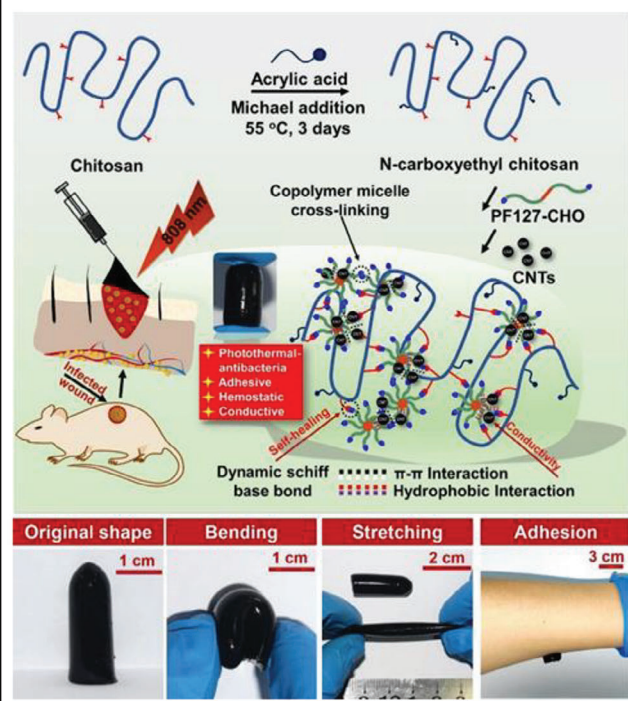
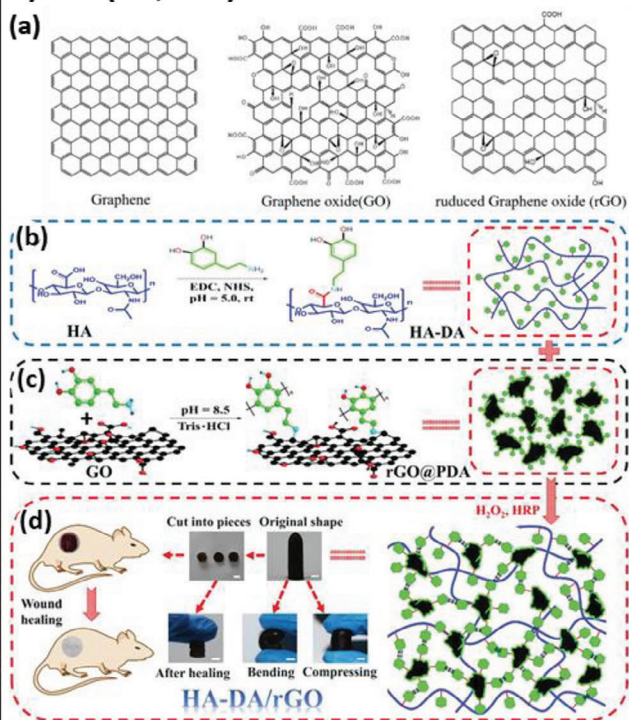
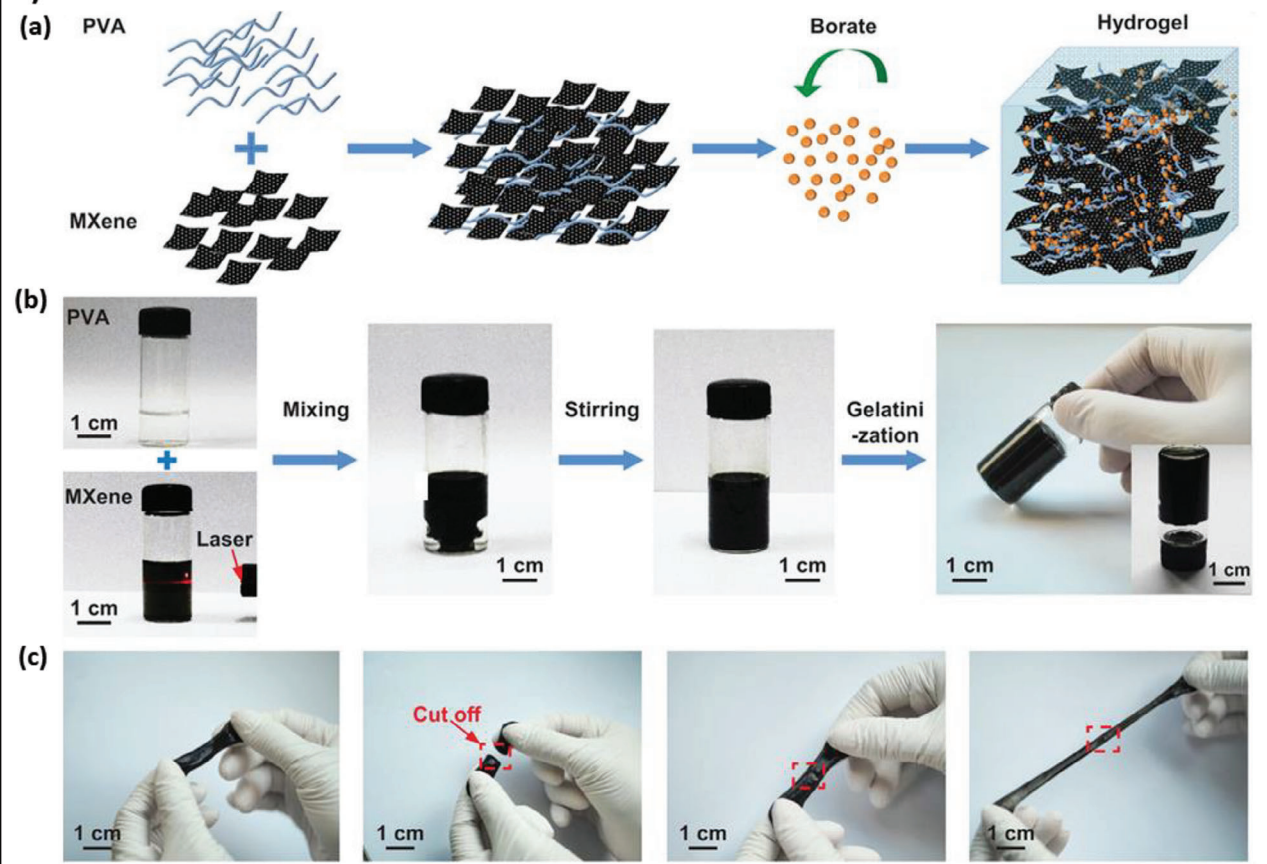
Furthermore, ZnO nanoparticles offer several advantages, such as high antibacterial efficacy at low concentrations (0.16–5.00 mmol L⁻¹), broad-spectrum activity against various strains, and relatively low cost.^[60] These nanoparticles can be synthesized using sol-gel synthesis from zinc salts, sol-gel combustion, chemical synthesis, low-temperature synthesis, and mechanical methods. Moreover, ZnO nanoparticles can interfere with microbial toxicity, leading to alterations in the expression of critical genes associated with cellular stress responses, motility, virulence, and toxin production.^[61] These nanomaterials are environmentally friendly and nontoxic, and Zn^{2+} ions released from ZnO nanoparticles move to the wound area, increasing the supply of zinc, which can facilitate skin tissue recovery and wound healing. ZnO has lower toxicity than other antimicrobial substances such as gold, silver, or titanium dioxide nanoparticles. Owing to its appropriate functionality in metabolism, the immune system, and wound-healing processes, nZnO is a vital source of Zn, which is an essential element for the human body.^[62] Despite concerns regarding nanoparticle toxicity in human health, nZnO has great potential for positive effects on wound healing.

2.3. Carbon-Based Conductive Polymers

In recent years, carbon-based materials such as CNTs, graphene oxide (GO), reduced graphene oxide (rGO), and activated carbon (AC) have garnered significant attention owing to their remarkable thermal, optical, electrical, and mechanical properties. These materials have attracted widespread interest in various fields.^[63]

2.3.1. Carbon Nanotube

There has been rapidly increasing interest in the development of CNT-based hydrogels. CNTs are carbon allotropes with high electrical and thermal conductivity.^[64] The unique properties of the CNT hybrid hydrogels are associated with the characteristics of the hydrogel polymer network. The CNT hybrid hydrogels were synthesized using five methods: 1) covalent crosslinking (*in situ* polymerization), 2) *ex situ* polymerization, 3) physical crosslinking, 4) polymer grafting, and 5) techniques enabled by intelligent devices.^[65] CNT materials are commonly combined with hydrogels to form electrically active composite dressings for wound-healing therapies. Adding CNTs to hydrogels provides the resulting composite with excellent electrical conductivity, enabling the effective delivery of electrical stimulation to wound tissues.^[66] For example, He et al. developed a hydrogel based on chitosan and CNT. The use of CNT-based composite dressing in the treatment of wounds showed significant downregulation of TNF- α expression and upregulation of VEGF expression, leading to accelerated wound healing^[67] (Figure 4A). These CNT-based

A) CNT-based CHs**B) GBN(GO, rGO)-based CHs****C) MXene-based CHs**

hydrogels exhibit outstanding antimicrobial properties, adhesion capabilities, antioxidative properties, and mechanical characteristics. As a result, this promising combination is widely used in wound healing and antimicrobial applications, activating local cell proliferation and migration.^[65,68] In another research, CNTs were integrated with chitosan and poly(acrylamide) (PAAm) to create a multifunctional hydrogel. This film was prepared to deliver VEGF and investigate the release pattern in the presence and absence of fluorescein isothiocyanate-tagged bovine serum albumin (FITC-BSA). The presence of CNTs enhances cellular interactions and proliferation.^[67]

2.3.2. Graphene Oxide

GO, formed by the oxidation of Gr (graphene), is a well-known and highly versatile material owing to its multifunctionality. It has gained popularity among researchers due to its wide surface area, π - π stacking, and potential for various applications.^[69] Graphene has been used in biomedical applications, including tissue engineering, owing to its excellent mechanical strength and electrical conductivity. They have applications in wound healing, stem cell engineering, regenerative medicine, and cellular growth and differentiation. This highly oxidized graphene monolayer contains a large number of oxygen-containing active groups such as carboxyl groups ($-\text{COOH}$), hydroxyl groups ($-\text{OH}$), carbonyl groups ($-\text{C=O}$), and epoxy groups ($-\text{O}-$).^[70] (Figure 4B). Carbonyl and carboxyl groups are predominantly located at the edges of GO. These groups exhibit excellent solubility and stability, making them suitable for cell-surface attachment, proliferation, and differentiation. GO possesses both hydrophobic and hydrophilic properties at the basal plane and edges, and contains oxygen-containing functional groups such as hydroxyl, epoxy, carbonyl, and carboxyl groups.^[70]

In addition, GO can be easily dispersed in water because of its hydrophilicity; however, its conductivity is lower than that of graphene. However, at weakly alkaline pH, dopamine can act as a reducing agent for GO, resulting in the formation of rGO and enhanced conductivity. Liang et al. fabricated conductive hydrogels based on dopamine-grafted hyaluronic acid (HA) and rGO through H_2O_2 crosslinking^[26] (Figure 4B). The enhanced conductivity of the hydrogel, achieved by incorporating rGO, enabled the transmission of electrical signals from viable tissues, stimulated cells that were responsive to electrical stimuli, and contributed to skin tissue regeneration. Free radicals in the wound area can induce oxidative stress, which leads to lipid peroxidation, DNA damage, and enzyme inactivation. Research on the local application of substances with free radical-scavenging properties in patients and animals has significantly improved wound healing. The excellent antioxidant capacity of the HA-DA/rGO hydrogel enhanced its potential for application in wound dressings.

2.3.3. MXene

MXenes have recently emerged as one of the most popular 2D materials owing to their elemental composition diversity, 2D transition metal carbides, wide surface area, abundant surface terminations, and excellent optoelectronic properties.^[71] The 2D structure also minimizes the migration distance between charge carriers and the reaction interface, inhibiting the possibility of charge carrier recombination, which improves the photocatalytic performance.^[72] The versatile chemistry of MXenes imparts interesting mechanical, electronic, magnetic, and electrochemical properties. In particular, the excellent flexibility of MXenes, coupled with their 2D morphology and layered structure, enables the easy formation of MXene-based composites, offering opportunities to integrate the exceptional characteristics of different materials in a complementary manner.^[73] Commonly synthesized MXenes include direct and indirect in situ HF etching.^[71] For hydrogel-based applications, MXenes offer an intriguing multifunctional platform for tissue regeneration in CHS (chronic wound-healing systems). The integration of MXenes into hydrogels has garnered particular interest because of their excellent mechanical strength, exceptional hydrophilicity, and diverse surface chemistry.^[74] MXenes have emerged as promising conductive nanofillers for polymer hydrogels with excellent multifunctional responsiveness. For instance, Zhang et al. prepared a self-healing MXene-PVA hydrogel by incorporating MXene into a polyvinyl alcohol (PVA) solution via borax crosslinking^[75] (Figure 4C). Their experimental results demonstrated that MXenes improved the conductivity of PVA hydrogels more effectively than CNTs under large strains. Furthermore, the hydrophilic groups of MXene, such as $-\text{OH}$, $-\text{O}$, and $-\text{F}$, enhance the self-healing capability of PVA hydrogels through increased hydrogen bonding. Furthermore, using MXenes as a dynamic crosslinking agent can result in excellent mechanical properties, adhesion, and self-healing capabilities. Ge et al. demonstrated the multifunctional role of MXenes in activating the rapid gelation of a wide range of hydrogels by controlling the dynamic interactions between MXenes and polymers.^[76]

3. The Effects of Electrical Stimulation on Wound Healing

The skin is composed of the dermis, epidermis, and stratum corneum, and is sensitive to electrical signals. Depending on various components, the skin exhibits a range of conductivity values, ranging from 2.6 to 1×10^{-4} mS cm $^{-1}$.^[77] Electrical stimulation therapy involves the use of two electrodes placed at different locations to allow a current to flow through the injured tissue. Depending on the direction of the current (or voltage), electrical stimulation can be divided into two types: unidirectional current (or voltage) and bidirectional current (or voltage).

Figure 4. Carbon-based CHs. A) Schematic representation of the CEC/PF/CNT hydrogel preparation showing the hydrogel's original shape, bending and stretching shape representations, and adhesion characteristics. Reproduced with permission.^[67] Copyright 2020, Elsevier. B) rGO-based CHs. a) Schematic diagram of GBNs. A diagram showing the creation of HA-DA/rGO hydrogel. b) HA-DA polymer preparation strategy with c) rGO@PDA, d) HA-DA/rGO hydrogel preparation scheme with original, bending, compression, self-healing representation, and application in wound healing. 5 mm scale bar. Reproduced with permission.^[26] Copyright 2019, Wiley-VCH GmbH. C) The process of making the MXene/PVA hydrogel. a) A diagram illustrating the creation of the MXene/PVA hydrogel. b) Photographs illustrating the preparation procedure of the MXene/PVA hydrogel. c) Photographs demonstrating the self-healability and stretchability of the prepared MXene/PVA hydrogel. Reproduced with permission.^[75] Copyright 2019, Wiley-VCH GmbH.

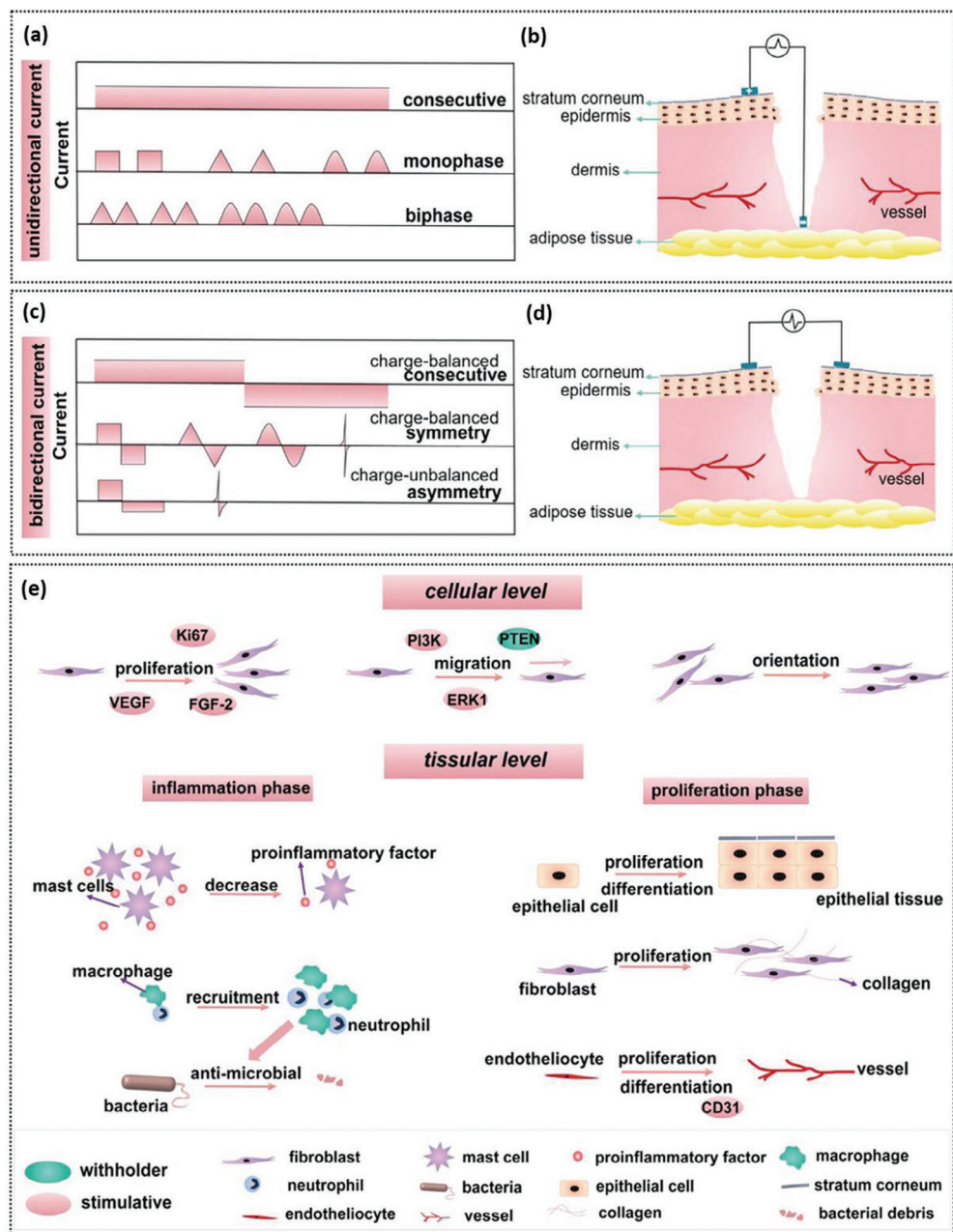


Figure 5. The waveform of electrical stimulation and the position of the electrode. a) Typical waveform of unidirectional current. b) When the electrical stimulation waveform is unidirectional current, the positive electrode is usually placed on intact skin, and the negative electrode is placed on the injured area. c) Typical waveform of bidirectional current. d) When the electrical stimulation waveform is bidirectional current, both electrodes are typically placed on intact skin. e) Effects of electrical stimulation on cellular and tissue levels: proliferation, migration, and inflammation. Reproduced with permission.^[78] Copyright 2021, Wiley-VCH GmbH.

Unidirectional currents include direct currents (DC) and unidirectional pulsed currents (PC). A unidirectional current is characterized by a one-way flow of charged particles, indicating consistent polarity (charge imbalance) (Figure 5a). This feature allows the simulation of an insulating electric field using a unidirectional current. Therefore, the anode of the electrical stimulation device is permanently attached to the intact skin around the wound, whereas the cathode is fixed at the center of the wound

(Figure 5b). However, the prolonged application of a unidirectional current to stimulate the wound can cause skin damage owing to thermal effects. Bidirectional current alternates polarity. When a bidirectional current stimulates a wound, the charged particles in the area beneath the electrodes alternate (Figure 5c). The two electrodes of the electrical stimulation device are typically placed on intact skin on either side of the wound (Figure 5d). Applying this current to a wound can significantly reduce or

3D Printing Conductive Polymer Hydrogels

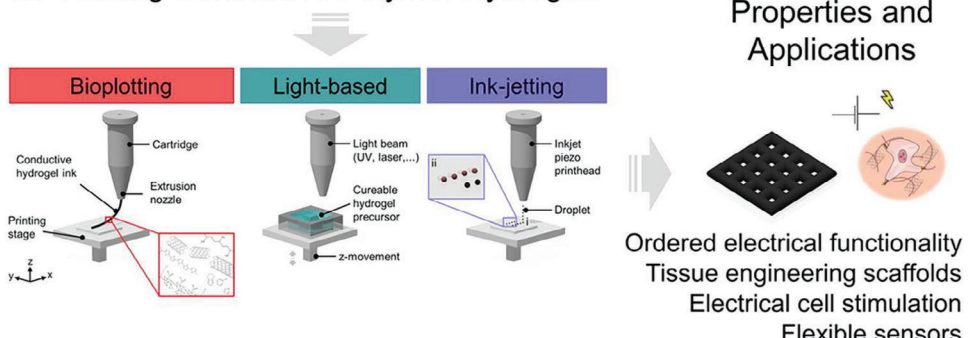


Figure 6. Schematic illustration of various types of 3D printing techniques. Reproduced with permission.^[81] Copyright 2020, Elsevier.

prevent thermal effects. Compared with unidirectional current, it has fewer side effects and is less invasive, making it a promising approach for clinical treatment. Regardless of the operating mode, both unidirectional and bidirectional currents affect wound healing in a similar manner (Figure 5e).^[78]

4. 3D Printing of Conductive Hydrogels

3D printing, also known as additive manufacturing (AM), is a computer-based technology that uses computer-aided design (CAD) data to replicate and create 3D objects through a layer-by-layer manufacturing process.^[79] The CAD figures were sliced into control units to direct the printers to build 3D structures.^[80] A 3D printer makes producing objects with complex shapes and designs more straightforward. In addition, it allows for customization, enabling the creation of products tailored to individual requirements. This flexibility has facilitated innovative designs and manufacturing processes in various industries. Conductive hydrogels have seen a surge in their utilization in 3D printing technology owing to their ability to produce customized structures with complex shapes and time-saving properties. 3D Printing is a comprehensive term that encompasses various digital-model-based layer-by-layer deposition technologies. This section introduces some prominent examples of light- and ink-based printing methods (Figure 6).

4.1. Light-Based 3D Printing

Light-based 3D printing is a layer-by-layer manufacturing process that offers excellent accuracy and resolution, intricate details, and a smooth surface finish. SLA and DLP are two standard techniques in light-based 3D printing, both of which involve immersing a build platform in a resin tank containing liquid resin and then building an object through successive layer depositions. These two techniques can be distinguished based on the light source used. SLA utilizes ultraviolet (UV) laser light, whereas DLP uses a digital light projector screen. One drawback of these photocuring 3D printing methods is volumetric shrinkage.

4.1.1. Stereolithography

Stereolithography (SLA) printing is based on the solidification of a liquid resin through photopolymerization. This technology has

immense potential for diverse applications and can be applied in various fields owing to its adaptable design and versatility. Generally, SLA printers use a 355 nm wavelength laser beam. The UV laser beam moves along the boundaries of the object and filled its 2D cross section. After one layer of resin is cured, the platform descends by one-layer thickness, and the curing process is repeated layer by layer to create a solid 3D object. The movement of the laser beam controls the formation of each layer. A laser beam can theoretically move over ample space, allowing SLA printers to print large objects.^[82] SLA technology enables the precise production of devices with complex shapes, high resolution, accuracy, precise details, and smooth surface finishes. However, a disadvantage of this technology is that the printing speed decreases as the object size increases, because of the curing speed associated with the movement of the laser beam. Heo et al. developed a photocrosslinking conductive hydrogel, including PEDOT:PSS, using an SLA 3D printer^[83] (Figure 7a). Patterned hydrogels exhibited decreased optical transparency and print diameter with increasing PEDOT:PSS concentration (Figure 7b). The mechanical properties of the conductive hydrogels were measured using a universal compression testing machine, and the compressive stress-strain curve showed that the strain increased with increasing PEDOT/PSS concentration (Figure 7c). Compressive stiffness decreased from 35.4 ± 1.4 to 26.3 ± 4.2 MPa as the PEDOT:PSS concentration (Figure 7d). In addition, the obtained conductive hydrogel increased the number of living cells with increasing PEDOT:PSS concentration (Figure 7e), indicating that the inclusion of PEDOT:PSS in the PEG hydrogel enhanced cell adhesion and promoted cellular proliferation.

4.1.2. Digital Light Projection

Digital light projection (DLP) technology uses the same principles as SLA. It involves the use of a digital projector to project a cross-sectional image of an object onto a light-sensitive liquid resin for polymerization. This printing method can operate in both the top-down and bottom-up configurations. The DLP technology projects the cross-sectional image of an object in a layer-by-layer manner across an entire platform. It simultaneously cures all points, offering the advantages of high precision and high manufacturing speed. The printing time for each layer remains the same regardless of the complexity or size of the

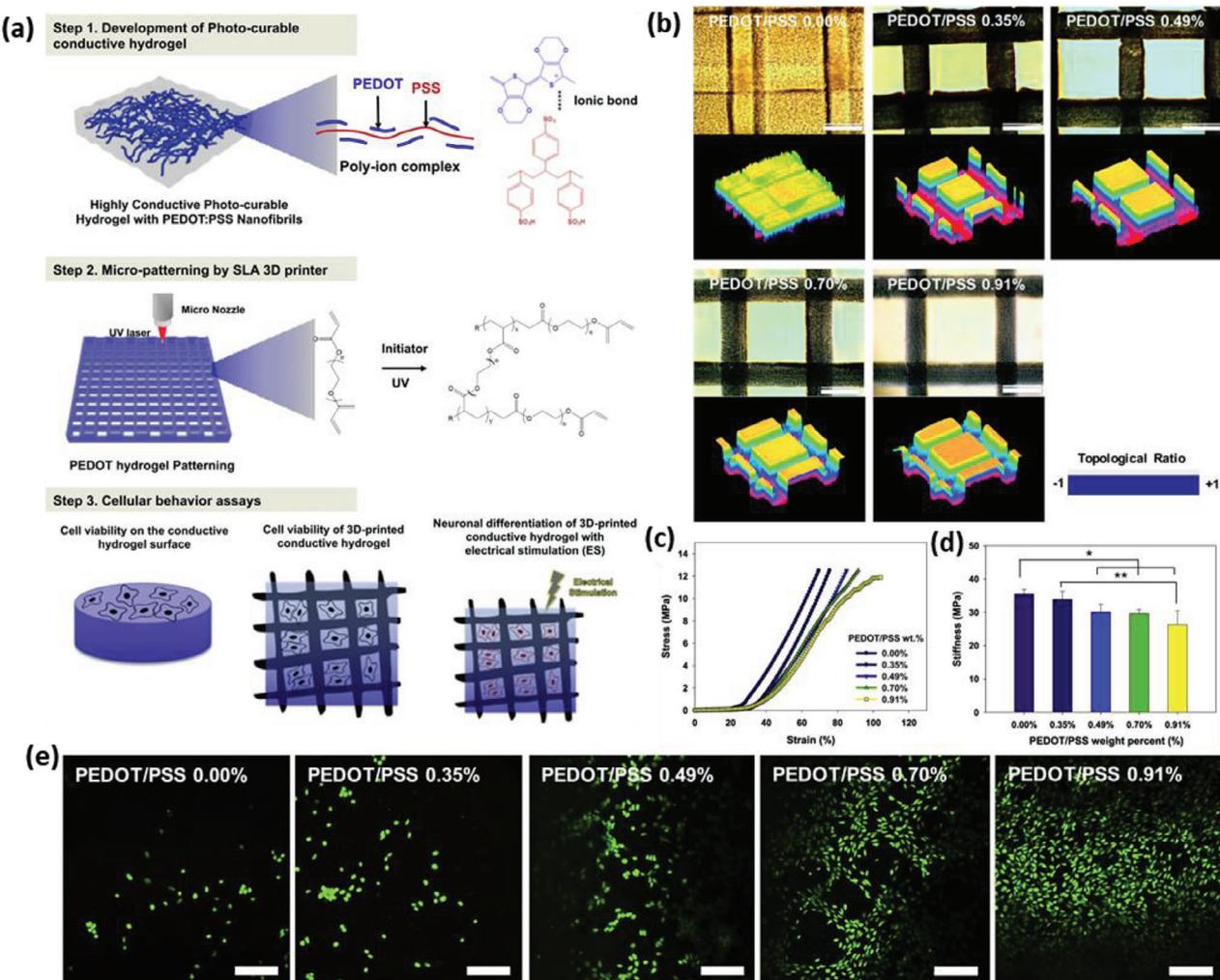
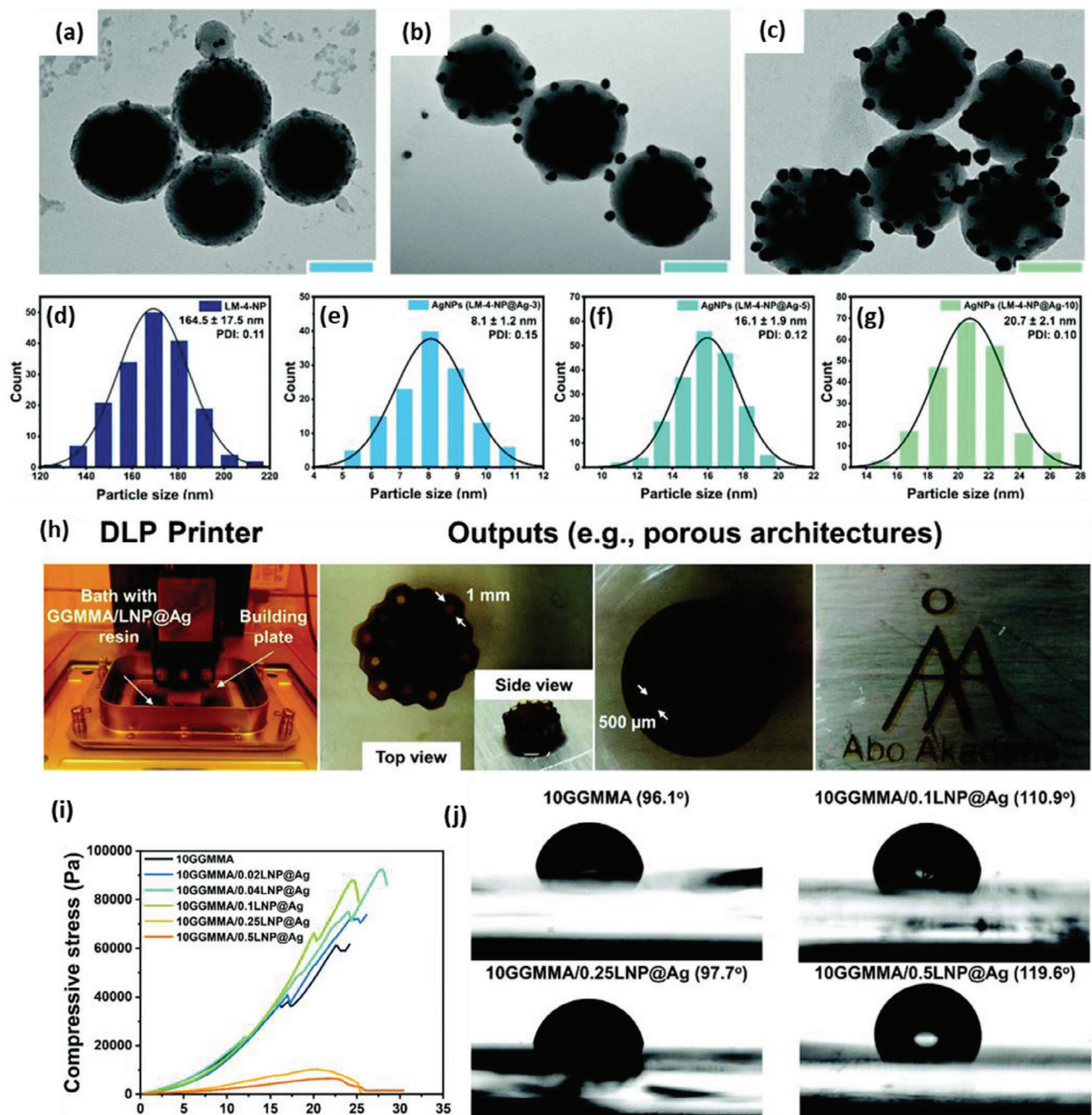


Figure 7. a) Overview of the process for manufacturing 3D conductive structures using the SLA printing system and cell behavior analysis. b) Optical and 3D surface plotting images displaying the hydrogel's diameter with the concentration of PEDOT/PSS. c) Hydrogel compression stress-strain curves based on PEDOT/PSS concentration. Stiffness (* $p = 0.05$ and ** $p = 0.01$, $n = 5$) is listed in (d). e) Live/dead experiment, in which the viability of a PEDOT/PSS hydrogel-coated dorsal root ganglion (DRG) cell culture was examined (* $p = 0.05$ and ** $p = 0.01$, $n = 5$). Copyright 2019, Reprinted with permission of *Materials Science and Engineering: C*. Reproduced with permission.^[83] Copyright 2019, Elsevier.

structure and depends only on the thickness of the object. These fast printing times and the nozzle-free approach ensured high cell viability (85%–95%).^[84] Furthermore, DLP printers require specific types of photosensitive resins for printing. These limitations in material selection restrict the use of various materials. Using the light-activation mechanism, a photosensitive resin must be combined or chemically modified with a photoinitiator. It is important to emphasize that the use of resin at inappropriate concentrations can harm the cells.^[85] Only a few photocrosslinkable biopolymers, such as gelatin, silk fibroin, and hyaluronic acid, which have been chemically modified with photoreactive moieties such as methacryloyl, have been employed as resins for DLP printing.^[86] Therefore, choosing safe ink materials and adhering to proper usage guidelines are crucial when using DLP printing.

To fabricate biomedical hydrogels using DLP printing, the current research focuses on the adaptability of bio-based resin compositions that provide suitable printability. Wang et al. created a

new antibacterial hydrogel containing inert spherical LNP carriers and surface-embedded AgNPs via DLP printing.^[87] The shape and size of the formed LNP@Ag were investigated by TEM (Figure 8a–c) and SEM measurements (Figure 8d–g). The antibacterial activity varied depending on the size of the AgNPs. The results of this study confirm that the size of the AgNPs formed in the LNP spheres depends on the concentration of the Ag precursor solution. In addition, the compression stress-strain curve showed that the mechanical rigidity of the GGMMA-based hydrogel was not significantly affected by the LNP@Ag content. Still, as the doping amount of LNP@Ag increased from 0.1 to 0.25 wt%, the stress during fracture decreased significantly (Figure 8i). The GGMMA/LNP@Ag hydrogel was manufactured by DLP additive manufacturing using a 10GGMMA/0.1LNP@Ag resin containing 0.25(w/v) % LAP photoinitiator (Figure 8h). Figure 8j shows that the increase in the hydrophobicity of the GGMMA surface after doping with LNP@Ag limits its binding to bacteria, resulting in an antibacterial effect.



4.1.3. Ink-Based 3D Printing

Ink-based 3D printing, also known as direct ink writing (DIW) or extrusion-based 3D printing, uses ink directly to precisely create objects. Both inkjet printing and DW systems have printer heads and focus on controlling the precise adjustment of ink and the layer-by-layer formation of objects. In addition, they require control over the drop formation speed, size, spacing, and fluid viscosity.

Ink-based 3D printing offers advantages such as versatility in material selection, the ability to print with multiple materials simultaneously, and the direct integration of functional elements or additives into printed objects. This technology has applications in various fields including biomedical engineering, electronics, art, and prototype manufacturing.

Inkjet Printing: Inkjet printing has emerged as a prominent extrusion-based printing technique and garnered significant attention as a manufacturing method for the deposition of

functional materials. It allows the use of various supply materials such as hydrogels, bioinks, and liquid polymers. Inkjet printing is characterized by its noncontact printing method, which makes it less susceptible to contamination, substrate, or mask damage and offers scalability.^[88] Industrial inkjet printing is highly flexible and robust. Inkjet-printing techniques are commonly categorized into two main types: continuous inkjet (CIJ) printing and drop-on-demand (DOD). In both methods, the liquid passes through an orifice or a nozzle; however, they differ in terms of the physical process of droplet formation. In CIJ printing, a liquid jet is subjected to force, which causes it to break up into a consistent series of droplets of uniform size and spacing owing to the influence of surface tension.^[89] The inherent breakup process driven by surface tension forces was further facilitated by controlling the flow rate through the nozzle at a suitable frequency. Usually, as the droplets traverse an electrostatic field, some acquire an electrical charge, directing them toward the intended position on the substrate and ultimately creating the desired printed image. The uncharged droplets were collected in a gutter for recycling. CIJ generates a high drop velocity ($>10\text{ m s}^{-1}$), which enables fast processing.^[88]

However, recycled ink is susceptible to contamination and may experience quality degradation after exposure to ambient conditions. In addition, compared with DOD, CIJ tends to have a lower resolution. By contrast, DOD printers selectively eject only the desired number of ink droplets from the print head and nozzles through thermal or piezoelectric operations. DOD printers are preferred over CIJ systems in most industrial fields, because they do not require drop charging, ink recirculation, or deflection. In a DOD printer, the liquid first emerges from the print head as a jet, and then detaches from the nozzle under surface tension forces, forming one or more droplets. After the droplets settle on the substrate surface, they dry by evaporation, leaving a solid deposit layer with a customized droplet deposition pattern.

Consequently, the deposited droplets can form “line” structures that can merge to form 2D planar sheets. Printing multiple layers of these sheets on top of one another results in 3D structures.^[90] DOD printers are preferred for applications involving high resolution, precision, excellent controllability, low cost, and scalability, particularly elastomers and biomaterials.^[91] Inkjet printing using conductive polymers has emerged as a promising technique for wound-healing and immunomodulatory applications. Conductive polymers, such as polyaniline, PEDOT:PSS, and polypyrrole, have unique electrical, mechanical, and biological properties that make them suitable for such applications.

In wound healing, inkjet printing can be used to create conductive scaffolds or films that mimic the ECM found in natural tissues. These scaffolds can be designed with specific patterns or geometries, allowing for precise control over the distribution of cells, growth factors, and other biomolecules. Furthermore, conductive polymers can facilitate electrical stimulation of cells, which has been shown to promote wound healing by enhancing cell migration, proliferation, and differentiation.^[92] The conductivity of these polymers also enables electrical signaling between cells, which plays a crucial role in tissue regeneration.

Regarding immunomodulation, inkjet printing can be used to create conductive polymer-based drug delivery and immunother-

apy platforms. These platforms can be designed to release drugs or immunomodulatory molecules in a controlled and localized manner by targeting specific immune cells or pathways.^[93] In addition, conductive polymers can be functionalized with ligands or antibodies that specifically bind to immune cells, thereby enhancing the targeting efficiency and efficacy of immunomodulatory treatments. Overall, inkjet printing using conductive polymers has excellent potential for wound-healing and immunomodulation applications. The ability to precisely control the structure and properties of printed materials combined with the unique characteristics of conductive polymers offers new opportunities for the development of advanced therapies and treatments for various diseases and conditions.

Direct Ink Writing: Among various AM technologies, DIW has emerged as the most versatile 3D printing technique for multiple materials. DIW is an extrusion-based printing method that enables the fabrication of 3D structures with complex medium- and microscale geometries and compositions.^[30] Because of its relatively gentle printing process, DIW is well suited for cell printing and a wide range of biological applications. DIW is also an extrusion-based printing method in which viscous polymer inks or pastes are extruded through a nozzle and then solidified through solvent evaporation, rapid homogenization, sol-gel transition, crosslinking, or post-treatment on the printed platform, forming solid layers on top of each other. The design and synthesis of ink materials play a crucial role in DIW technology. To achieve shape fidelity, ink materials must exhibit high elasticity before extrusion, demonstrate good shear-thinning behavior as they pass through tiny nozzles, and regain their high elasticity after deposition. These characteristics depend heavily on the chemical structure and composition of the ink.^[94] The machine parameters, including the nozzle size and printing speed, affect the printing accuracy and resolution. Generally, smaller nozzle diameters can improve the printing resolution. However, a higher extrusion pressure and longer build time may be required to prevent nozzle clogging.

Similarly, lower printing speeds usually result in improved dimensional tolerance and fidelity; however, the printing time increases. The uniqueness of the printing process lies in its ability to extrude continuous filaments at room temperature. Printability depends on the rheological properties of the ink rather than its temperature dependence.^[95] The key advantages of DIW include its ability to select a wide range of materials (polymers, colloidal dispersions, hydrogels, etc.), adjustable viscosity (10^2 – 10^6 mPa s), rapid prototyping (1 mm s^{-1} to 10 cm s^{-1}), and cost-effectiveness.^[80,95] In addition, DIW offers short manufacturing times, high mechanical and electrical performance of printed parts, and virtually no limitations on geometric structures.^[96] DIW has some drawbacks. First, the inevitable ink spreading caused by gravity deteriorates the shape fidelity of the printed object.^[80] In addition, compared with the light used in SLA, the movement of the nozzle in DIW is slower, necessitating further improvements in the printing speed. Moreover, DIW is limited by its high cost, excessive oxidation caused by lasers, and residual stress in the fabricated parts.^[97] Creating functional and conductive hydrogels using the DIW technique is challenging because of complex ink formulation and printing processes. Liu et al. fabricated 3D-printed PEDOT:PSS/CNT-based hydrogels by freeze-thawing and H_2SO_4 treatment^[98] (Figure 9a). By

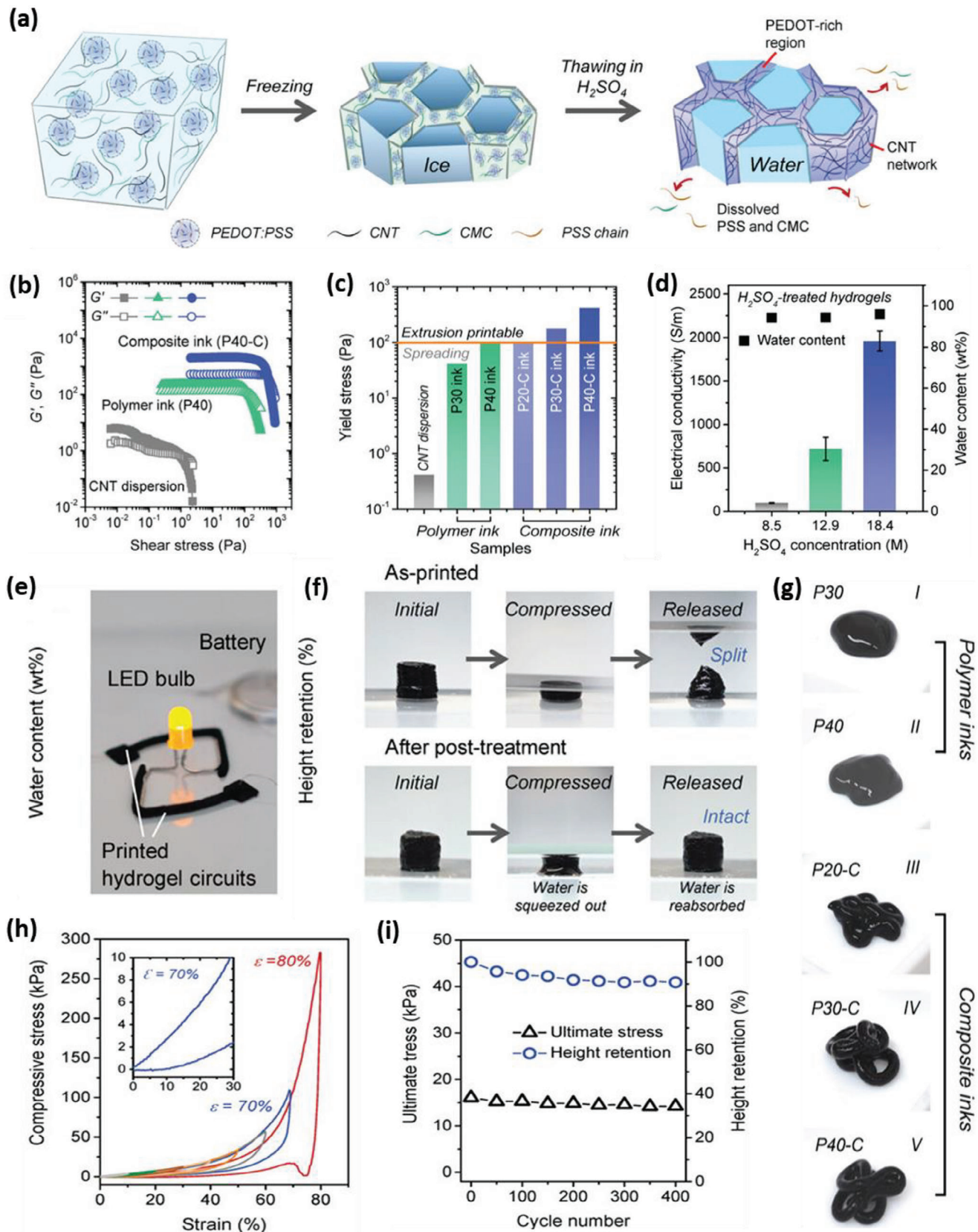


Figure 9. a) A schematic diagram describing the gelation process during post-printing. b,c) The moduli and yield stresses of different inks (the polymer and composite inks were termed as P_x and P_x-C , respectively, where x represents the PEDOT:PSS concentration ($mg\text{ mL}^{-1}$) in the ink, and C indicates

using a CNT dispersion to dissolve the PEDOT:PSS, the modulus and yield stress of the synthesized ink increased significantly (Figure 9b,c), allowing the deposited ink filaments to maintain a stable shape during the printing process without collapsing (Figure 9g). The 3D-printed hydrogels achieved high electrical conductivity of $\approx 2000 \text{ S m}^{-1}$ with a water content of 96.0 wt% (Figure 9d,e). Compression tests revealed that the post-treated hydrogels exhibited high elasticity, rapidly recovering their original shape even at 10%–80% deformations (Figure 9f–h). The hydrogels exhibited excellent fatigue resistance, maintaining a height deformation of $\approx 9\%$ after 400 compression cycles at a strain of 30% (Figure 9i). These remarkable mechanical properties can be attributed to the interaction between the CNTs and PEDOT: PSS as well as the structural characteristics of the hydrogels.

5. 3D Printed Conductive Hydrogels for Macrophage Polarization

Stimuli-responsive hydrogels have shown great potential in various fields such as soft robotics, biomedicine, and flexible electronics. These hydrogels can change their properties, such as shape and volume, in response to external stimuli, including temperature, pH, light, and electric and magnetic fields.^[99] In recent years, there has been increased interest in the development of electrical stimuli-responsive hydrogels for their potential applications in triggering macrophage polarization to angiogenesis.^[100] Macrophage polarization refers to the process by which macrophages, a type of immune cell, undergo functional and phenotypic changes in response to specific environmental signals. One potential application of electrical stimuli-responsive hydrogels is in the field of bioengineering, where they can be used to modulate macrophage polarization and promote angiogenesis. To understand the mechanism by which 3D printable hydrogels trigger macrophage polarization for angiogenesis, it is important to understand the concept of macrophage polarization. Macrophage polarization refers to the process by which macrophages adopt different functional phenotypes in response to specific environmental signals. These signals can be classified into two main types: M1 and M2. M1 macrophage polarization is associated with pro-inflammatory responses^[101] and tissue destruction, whereas M2 macrophage polarization is associated with anti-inflammatory responses and tissue repair. Previous studies have shown that modulating macrophage polarization toward the M2 phenotype can promote angiogenesis and tissue regeneration. Electrical stimuli-responsive hydrogels represent a novel approach for triggering macrophage polarization toward the M2 phenotype and promoting angiogenesis. Electrical stimuli-responsive hydrogels can be engineered to release specific electrical signals that mimic physiological signals present in the microenvironment and trigger macrophage polarization.

the use of CNT dispersion to dissolve the PEDOT:PSS, respectively). d) Water contents and electrical conductivities of hydrogels treated with various concentrations of H_2SO_4 . e) Photographs of the hydrogel as a conductor to light up an LED bulb. f) Photographs showing the compressibility of hydrogel printed before and after processing. g) Visualized photographs of pure polymer ink and composite ink extruded from syringes. h) Circular compression curve of hydrogel printed at strain rate from 10% to 80%. i) The printed hydrogel's extreme stress and relative height for 100 compression cycles. Reproduced with permission.^[98] Copyright 2023, Wiley-VCH GmbH.

5.1. Role of Macrophage Polarization during Wound Healing

Macrophages are critical players in the immune response and tissue repair processes. They can switch between different phenotypes, allowing them to dynamically perform diverse functions. Macrophages orchestrate the complex process of blood vessel formation during angiogenesis and skin tissue regeneration. Macrophages facilitate angiogenesis by secreting factors that promote blood vessel growth and maturation. M1 macrophages are responsible for the initiation of angiogenesis, as they secrete vascular endothelial growth factor that stimulates the proliferation and migration of endothelial cells.^[100] In contrast, M2 macrophages are involved in the later stages of angiogenesis and are responsible for stabilizing blood vessels.^[100]

Furthermore, M2 macrophages secrete the platelet-derived growth factor-BB, which promotes the maturation and stabilization of blood vessels. Incorporating electrical stimuli-responsive hydrogels into the macrophage polarization and angiogenesis fields offers a promising approach for enhancing tissue regeneration. By utilizing electrical stimuli-responsive hydrogels, researchers can precisely control and modulate the release of specific electrical signals to trigger macrophage polarization toward the M2 phenotype, which is associated with angiogenesis and tissue regeneration. In a study by Li et al., electrical stimuli-responsive hydrogels were developed and incorporated into scaffolds to promote both osteogenesis and angiogenesis by guiding macrophage polarization toward the M2 phenotype and promoting the release of antigenic factors.^[100] The researchers found that incorporating TGF- β 1 into the hydrogel could guide macrophage polarization toward the M2 phenotype.^[100] This results in the secretion of factors that promote angiogenesis, such as the vascular endothelial growth factor, and enhances blood vessel formation within the scaffold.

Moreover, researchers observed that the electrical stimuli-responsive hydrogel enhanced osteogenesis, suggesting its potential for promoting overall tissue regeneration. Li et al. highlighted the potential of electrical stimuli-responsive hydrogels in triggering macrophage polarization toward the M2 phenotype and promoting angiogenesis. Electrical stimuli-responsive hydrogels that trigger macrophage polarization toward the M2 phenotype and promote angiogenesis hold great potential for tissue regeneration and regenerative medicine.^[102] By precisely controlling the release of electrical signals, these hydrogels can guide macrophages to adopt the M2 phenotype, thereby promoting angiogenesis and tissue regeneration. Furthermore, incorporating electrical stimuli-responsive hydrogels into scaffolds offers a unique advantage by providing spatial and temporal control over macrophage polarization and angiogenesis. This control allows for the targeted delivery of antigenic factors and the modulation of macrophage behavior, ultimately leading to enhanced tissue regeneration. Previous studies have demonstrated the

effectiveness of modulating macrophage polarization and promoting angiogenesis using different types of scaffolds.

5.2. Impact of Electrical Stimuli and 3D Printed Hydrogels for Enhancing Angiogenesis and Skin Tissue Regeneration

The development of electrical stimuli-responsive hydrogels for tissue regeneration has shown promising results in the promotion of angiogenesis. These hydrogels can effectively guide macrophage polarization toward the M2 phenotype by utilizing electrical signals that play crucial roles in angiogenesis and tissue regeneration.^[102] This advanced control and modulation of macrophage behavior and angiogenesis significantly promotes tissue regeneration, especially in skin tissue. Skin tissue regeneration often requires the formation of blood vessels to support the growth and development of new tissues. The ability of electrical stimuli-responsive hydrogels to promote angiogenesis by triggering macrophage polarization toward the M2 phenotype addresses this challenge. This offers new opportunities for developing advanced skin tissue regeneration strategies.^[102]

Moreover, using 3D printable hydrogels further enhances the potential of electrical stimuli-responsive systems in tissue regeneration. These hydrogels can be precisely designed and printed into complex 3D structures to create personalized scaffolds that mimic the architecture and functions of native tissues. In addition, the incorporation of electrical stimuli responsiveness into these hydrogels adds another layer of control and adaptability. For instance, by applying electrical stimuli to a hydrogel scaffold, macrophage polarization can be manipulated in real time, promoting a proangiogenic microenvironment and enhancing tissue regeneration.^[102] Furthermore, studies have shown that the type of hydrogel used can influence macrophage polarization and angiogenesis. For example, electrospun poly scaffolds have been found to exhibit greater angiogenic properties and M2 macrophage polarization compared to electrospun poly- ϵ -caprolactone scaffolds. In addition, polyhydrogels with a pore size of 30–40 μm have been found to stimulate angiogenesis, reduce fibrotic response, and promote macrophage shift toward the M2 phenotype. This suggests that by carefully designing and controlling the properties of these hydrogels, researchers can effectively promote tissue regeneration and formation of new blood vessels. The ability to modulate macrophage polarization through electrical stimuli-responsive 3D printable hydrogels opens new possibilities for tissue regeneration and angiogenesis strategies.^[102] These hydrogels offer a targeted and precise approach for controlling the behavior of immune cells, specifically macrophages, which play a crucial role in tissue homeostasis and regeneration.^[102,103] Using electrical stimuli-responsive 3D printable hydrogels to trigger macrophage polarization to angiogenesis is a promising avenue for tissue regeneration. This approach could potentially revolutionize regenerative medicine by providing a novel and effective method for promoting angiogenesis and tissue remodeling. Further research is needed to fully understand the underlying mechanisms and factors responsible for the observed effects of electrical stimuli-responsive hydrogels on macrophage polarization and angiogenesis. Overall, research on electrical stimuli-responsive 3D printable hydrogels as

a means of triggering macrophage polarization to angiogenesis is promising.

6. Biomedical Applications

The application of 3D-printed conductive hydrogels has emerged as a promising technology in biomedical engineering. By combining the unique properties of high water content and biocompatibility with the inherent conductivity of the embedded materials, hydrogels offer versatile possibilities for various therapeutic strategies. One of the key applications of 3D-printed conductive hydrogels is in wound healing. These hydrogels possess conductivity that can facilitate the wound-healing process. This section elaborates on some examples of commercially available hydrogel-based wound dressings (Table 2). They can also be used for immunomodulation and drug delivery.

6.1. Wound Healing and Immunomodulation

The skin is the first barrier that protects the body from the external environment. Extensive skin damage caused by mechanical injuries, burns, or diabetes often impairs skin function and leads to scarring. Wound healing and skin tissue regeneration have become popular research topics in regenerative medicine. Wound healing involves four stages: hemostasis, inflammation, proliferation, and remodeling. Traditional wound dressings have the disadvantages of insufficient hemostatic and antimicrobial effects. Hydrogels with excellent biocompatibility, biodegradability, tunable mechanical strength, and high oxygen and moisture permeability have gained attention as alternatives to address these issues.^[11,110] A hydrogel is a 3D crosslinked hydrophilic polymer biomaterial that can absorb a large amount of water and maintain a moist environment, making them ideal materials for dry wounds.^[110] Hydrogels allow the passage of oxygen and water vapor, maintain a moist environment, reduce wound temperature, and provide pain relief. 3D-printed hydrogels demonstrate outstanding potential in tissue engineering for fabricating cell culture scaffolds owing to their similarity to the ECM. Hydrogels have received considerable attention owing to their ability to gel in the field depending on the shape of the wound. Conductive hydrogels have emerged as tools for wound healing. Integrating electrical activity into hydrogels allows for the upregulation of cellular activities and behaviors.^[111] ES can provide wound relief, induce keratinocyte migration, enhance reepithelialization, and promote angiogenesis around electrodes, triggering the release of pharmacological and other physiologically active molecules.^[112] This strengthens intercellular signaling, enhances blood circulation, and stimulates cell proliferation, thereby promoting wound healing and tissue regeneration.

For example, Lee et al. used a DLP printer to fabricate a conductive GelMA/PEDOT:PSS scaffold with microgrooves and combined electrical stimulation to promote wound regeneration^[8a] (Figure 10a). The aligned groove pattern on the scaffolds functioned as a bridge, guiding cellular migration and proliferation, and consequently enhancing their regeneration and migration rates (Figure 10c,d). The excellent electrical conductivity of this scaffold enhanced the cellular proliferation and improved

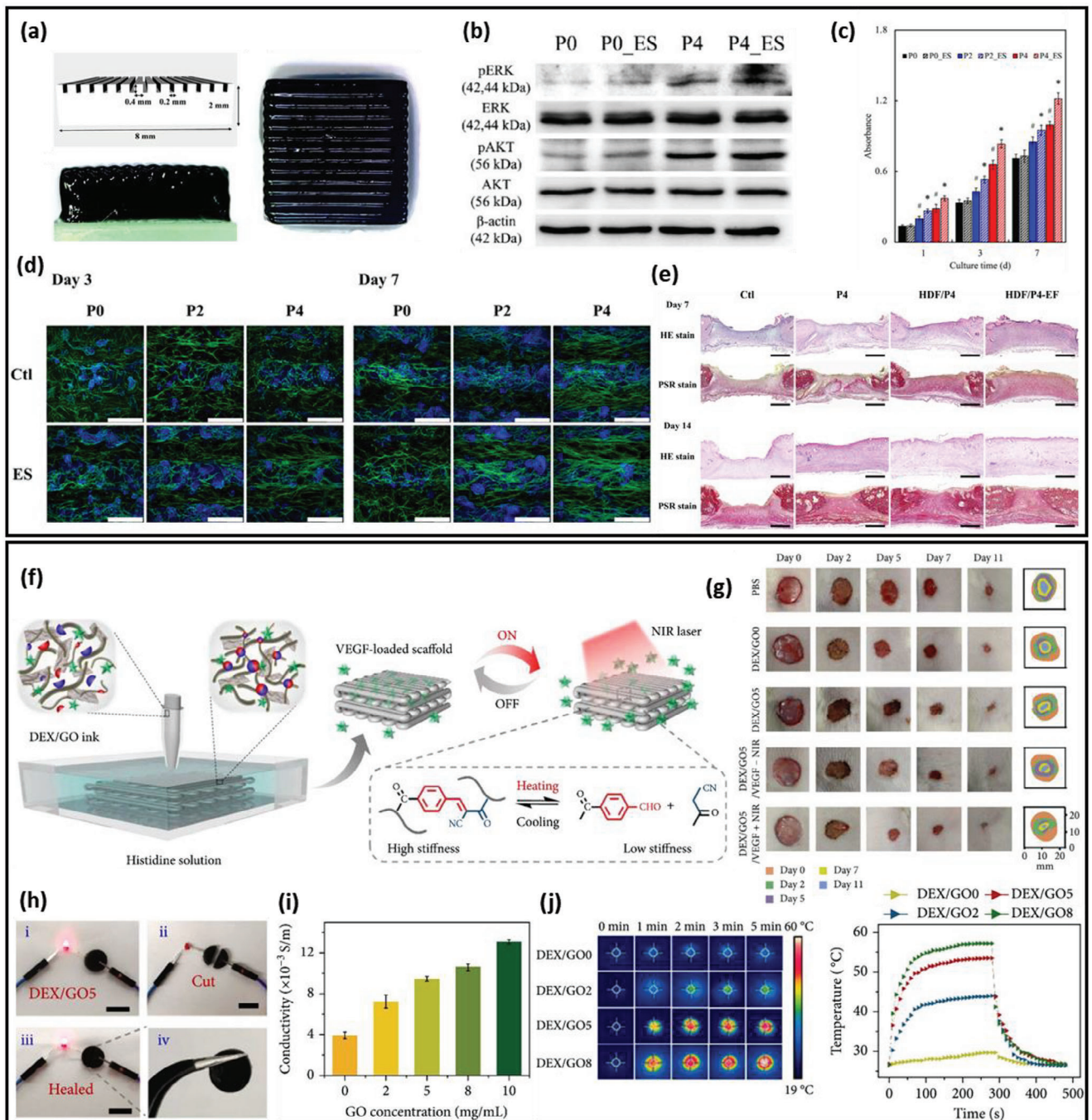


Figure 10. a) Photograph of the GelMA/PEDOT:PSS scaffolds containing grooves and ridges pattern on the surface using software. b) The mechanism by which the conductive hydrogel promoted skin regeneration in vitro. The proteins expression of ERK, p-ERK, AKT, p-AKT, and β -actin for HDF cultured on P0 and P4 scaffolds and treated with electrical stimulation considered using a western blot. c) Proliferation rate of HDF cultured on the GelMA/PEDOT:PSS scaffolds and treated with electrical stimulation for different numbers of days. The scale bar is 500 μ m. Data presented as mean \pm SEM, $n = 6$ for each group. # indicates a significant difference ($p < 0.05$) from P0. * indicates a significant difference ($p < 0.05$) from the scaffold without electrical stimulation (ES). d) F-actin/nuclei staining. e) Hematoxylin and eosin (H&E) and picrosirius red (PSR) staining used to evaluate new skin regeneration in the critical-sized defect *in vivo* 7 and 14 d after implantation. Reproduced with permission.^[8a] Copyright 2022, Elsevier. f) Preparation and NIR-induced stiffness change of the GO hybrid hydrogel scaffold. g) Wound images in rats after treatment. h) Optical images demonstrating the good conductivity of the 8% DEX/GO5 hydrogel during a breaking/healing cycle. Scale bars: (i–iii) 1 cm. i) The conductivity of the 8% hydrogels with different GO contents. j) Thermo-responsive cycles of the hybrid hydrogel with different GO contents and the corresponding real-time infrared thermal imaging pictures. Reproduced with permission.^[113] Copyright 2022, Elsevier.

Table 2. Characteristics of hydrogel-based wound dressings.^[115]

3D printing methods	Principle	Materials	Accuracy [μm]	Resolution [μm]	Ref.
Digital light processing (DLP)	Photocuring by a digital projector	Photopolymer and photoresin	10–25	x: 25 y: 25 z: 20	[104]
3D inkjet printing	Extrusion of ink and powder liquid combinations	Photoresin or hydrogel	100	x: 10 y: 10 z: 50	[105]
Selective laser sintering (SLS)	Laser-induced manipulation of powder particles	Polyamide, PVC, metallic powder	300	x: 50 y: 50 z: 200	[106]
Polyjet	Droplet deposition and hardening of photocurable liquid materials	Polymer	10–20	x: 30 y: 30 z: 20	[107]
Stereolithography (SLA)	Cross-sectional area by UV-initiated polymerization cross-sectional area	Resin (based on acrylate or epoxy with dedicated photoinitiator)	25–150	x: 10 y: 10 z: 15	[108]
Fused deposition modeling (FDM)	Constant filament extrusion	Nylon, PLA, wax blend, ABS	350	x: 100 y: 100 z: 250	[109]

the migration and orientation of human epidermal fibroblasts (Figure 10b). The presence and proliferation of essential cells such as keratinocytes, fibroblasts, and endothelial cells play a crucial role in wound remodeling during wound healing, and this process can be enhanced by electrical stimulation (Figure 10e).

In another study, a hydrogel with high conductivity, high photothermal conversion efficiency, excellent biocompatibility for wound healing, and antibacterial properties was developed by incorporating GO, a conductive material^[113] (Figure 10f). The scaffolds printed using the glass capillary microfluidic 3D printing technique demonstrated improved electrical conductivity (Figure 10h,i), enhanced mechanical properties, and superior photothermal performance owing to the presence of GO (Figure 10j). Furthermore, a GO hydrogel loaded with VEGF promoted wound healing and angiogenesis in a debrided full-thickness skin wound model, demonstrating its potential for biomedical applications (Figure 10g).

Immune cells play a pivotal role in wound healing. These cells promote stem cell proliferation and neovascularization.^[114] Macrophages secrete inflammatory factors that significantly affect tissue regeneration in damaged areas. The overall inflammatory response during the early stages of wound healing helps prevent infection of the damaged tissue. The initial inflammatory reaction has a positive effect on wound healing, whereas the later stages of healing promote tissue repair.

Mature macrophages are classified into pro-inflammatory M1 and anti-inflammatory M2 subtypes through polarization, and are influenced by pro-inflammatory and anti-inflammatory cytokines (Figure 11). M1 macrophages are predominantly present in the early stages of wound healing, and exhibit increased secretion of inflammatory including interleukin (IL)-1, IL-6, IL-12, tumor necrosis factor-alpha (TNF- α), and reactive metabolites. The anti-inflammatory cytokine IL-10 secreted by M2 macrophages plays a crucial role in suppressing inflammatory mediators and promoting wound healing.^[115] Approximately 5 d after injury, the polarization of macrophages into an M2-like phenotype oc-

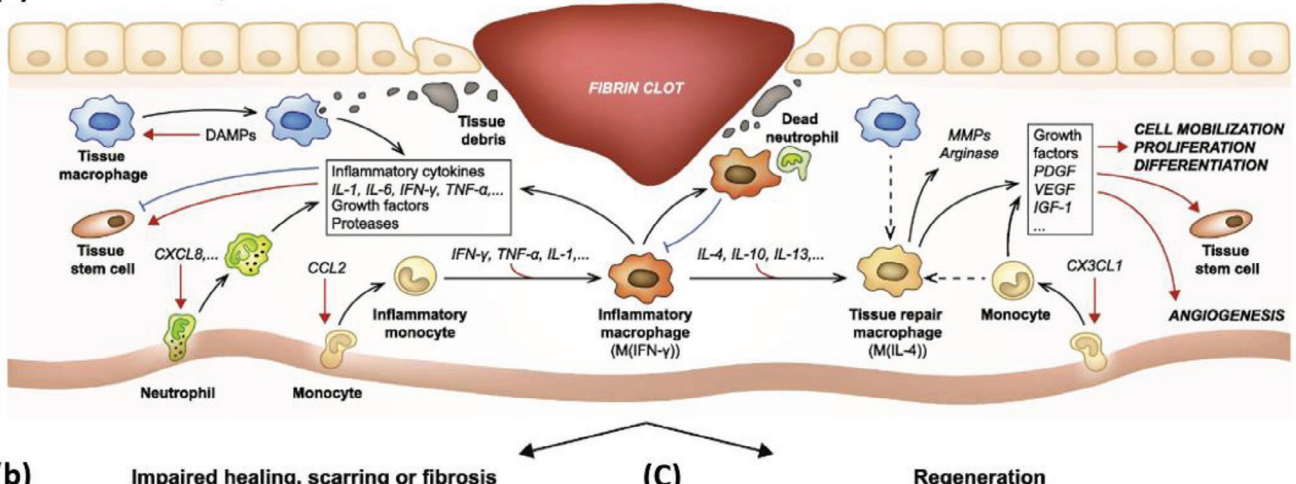
curs due to the secretion of Th2 cytokines, such as IL-4, IL-13, and IL-10. This transition signified a shift from the inflammatory phase to the healing phase. The M2 macrophages replace the M1 macrophages and play a significant role in late-stage tissue repair. They limit local inflammation, promote anti-inflammatory fibrosis, and facilitate the generation of angiogenic mediators, thereby facilitating tissue recovery.^[103]

Cao et al. developed wound dressings composed of ROS-responsive polyurethane membranes loaded with DOXH (Doxorubicin hydrochloride) and 3D-printed conductive hydrogel strips^[117] (Figure 12a,b). These dressings are based on the unique properties of hydrogels and drug-loaded membranes to promote skin regeneration through antimicrobial, ROS scavenging, conductivity, and immune-modulating capabilities. Chronic diabetic wounds fail to transition from the inflammatory phase to the proliferative phase, and one of their characteristics is the dysregulation of the M1/M2 phenotype ratio. High levels of inflammatory factors such as ROS, TNF- α , and IL-1 β are sustained, destroying normal and regenerating tissues. In contrast, M2 macrophages possess anti-inflammatory and tissue regeneration-promoting properties. DOXH promotes macrophage polarization toward the M2 phenotype (Figure 12c,d). Wounds treated with MD-H and MD-CH dressings showed a significantly higher ratio of CD206-positive M2 macrophages to CD68-positive M1 macrophages, indicating that DOXH can effectively regulate the polarization of macrophages toward the M2 phenotype in diabetic wounds (Figure 12e,f). Therefore, DOXH plays a crucial role in diabetic wound regeneration by regulating the dysfunctional wound microenvironment through ROS scavenging and promoting macrophage polarization toward the M2 phenotype.

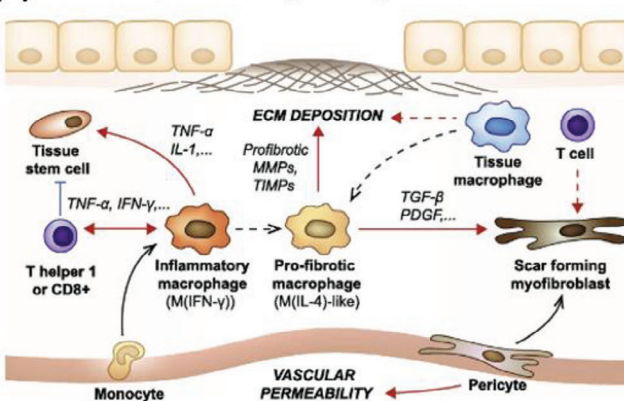
6.2. Application of Drug Delivery

In tissue engineering, 3D-printed scaffolds are widely used as drug delivery systems. Various types of hydrogel scaffolds that

(a) Initial immune response



(b) Impaired healing, scarring or fibrosis



(C)

Regeneration

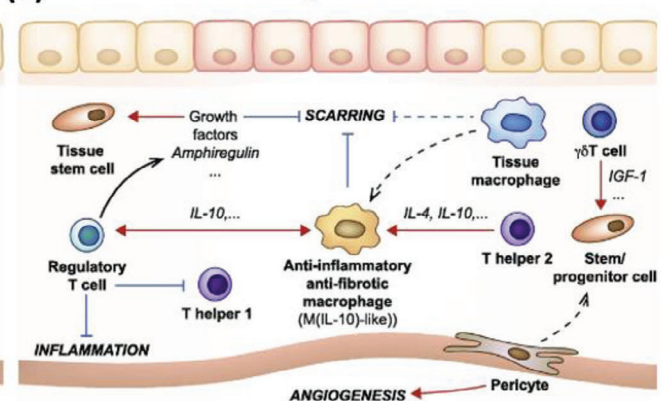


Figure 11. a) Overview of the first phase of inflammation after tissue injury. Pro-inflammatory M (IFN- γ) macrophages initially maintain the inflammatory response, which is subsequently suppressed with the help of M (IL-4) macrophages. b) A description of the immunological processes that can impair tissue recovery or cause scarring and fibrosis. A description of the immunological processes that can impair tissue recovery or cause scarring and fibrosis. Reproduced with permission.^[116] Copyright 2017, Elsevier.

can release drugs triggered by external stimuli such as magnetic fields, near-infrared (NIR) laser irradiation, and ultrasound have been reported.^[118] Examples of various stimuli-responsive conductive hydrogels with their optimized dose for drug delivery is given in **Table 3**.

However, drug-loaded hydrogels are generally unsuitable for long-term drug delivery because of uncontrolled diffusion of

drugs from swollen hydrogels. Liu et al. developed hydrogels by sequentially coating PCL and PDA onto 3D-printed alginate/gelatin scaffolds^[124] (**Figure 13a**). The encapsulation of PCL effectively reduced gel swelling and prevented uncontrolled diffusion of drugs. Owing to its good biocompatibility and photothermal conversion effects, PDA induced a temperature increase in the system under NIR irradiation (**Figure 13b**), leading to a

Table 3. Stimuli-responsive conductive hydrogels for smart drug delivery

Type of stimulus	Scaffold/hydrogel platform	Stimulus parameters	Drug release [%]	Application	Ref.
Magnetic fields	β -CD/cellulose hydrogel	400 Oe	58	Implantable smart drug delivery vehicles	[119]
NIR laser irradiation	GelPV-DOX-DBNP hydrogel	660 nm	73	Chemo-photothermal combination therapy against the cancers	[120]
Ultrasound	(DS@PEG-PLGA)@PEG hydrogel patch	2 W cm ⁻²	47	Treating diseases such as arthritis and topical soft tissue injuries	[121]
UV	OAL-CS hydrogel	4 mW cm ⁻²	96	Smart drug control release	[122]
Electrical stimulus	rGO-PVA hydrogel	15 V	64.99	Transdermal therapy, wound healing	[123]

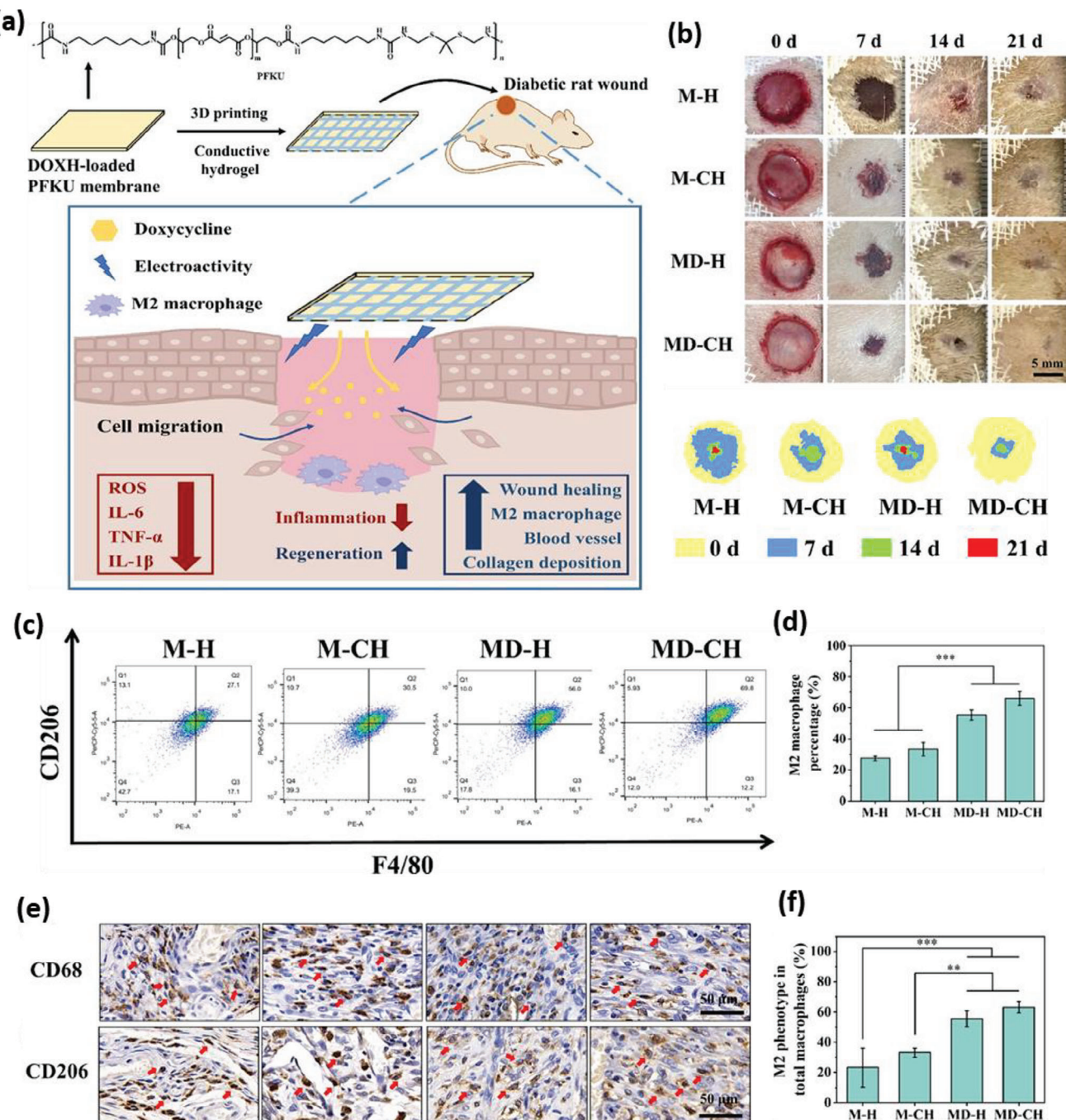


Figure 12. a) Overall schematic diagram of a composite dressing consisting of conductive hydrogel strips and PFKU fibrous membrane containing DOXH for diabetic wound healing based on immunomodulatory ability. b) Overlay images showing the wound status of different groups at 0, 7, 14, and 21 d post-injury. c,d) Polarization of M2 (F4/80⁺ and CD206⁺ stained) macrophages cultured from various wound dressings evaluated through flow cytometry. e) Representative immunohistochemical staining images of CD68 and CD206 at 7 d after wound treatment showed positive cells in brown color. f) Percentage of CD206/CD68-positive M2 macrophages at the wound site on the seventh day. (*, **, and *** represent $P < 0.05$, 0.01 , and 0.001 , respectively.) Reprinted with permission.^[117] Copyright 2022, Elsevier.

sol-gel transition of the core gels and facilitating drug release from the loosened hydrogel matrix. This PCL coating decreased drug diffusion, enabling sustained drug release over an extended period (Figure 13c-f). Moreover, functional hydrogels that respond to external stimuli have significant advantages as precise

drug delivery systems. These hydrogels enhance the efficacy of drugs and minimize side effects, while localized drug delivery reduces dosage and treatment costs.^[125] Qu et al. developed a biocompatible conductive hydrogel based on dextran and aniline trimers as an electroresponsive drug delivery system.^[126] Dextran

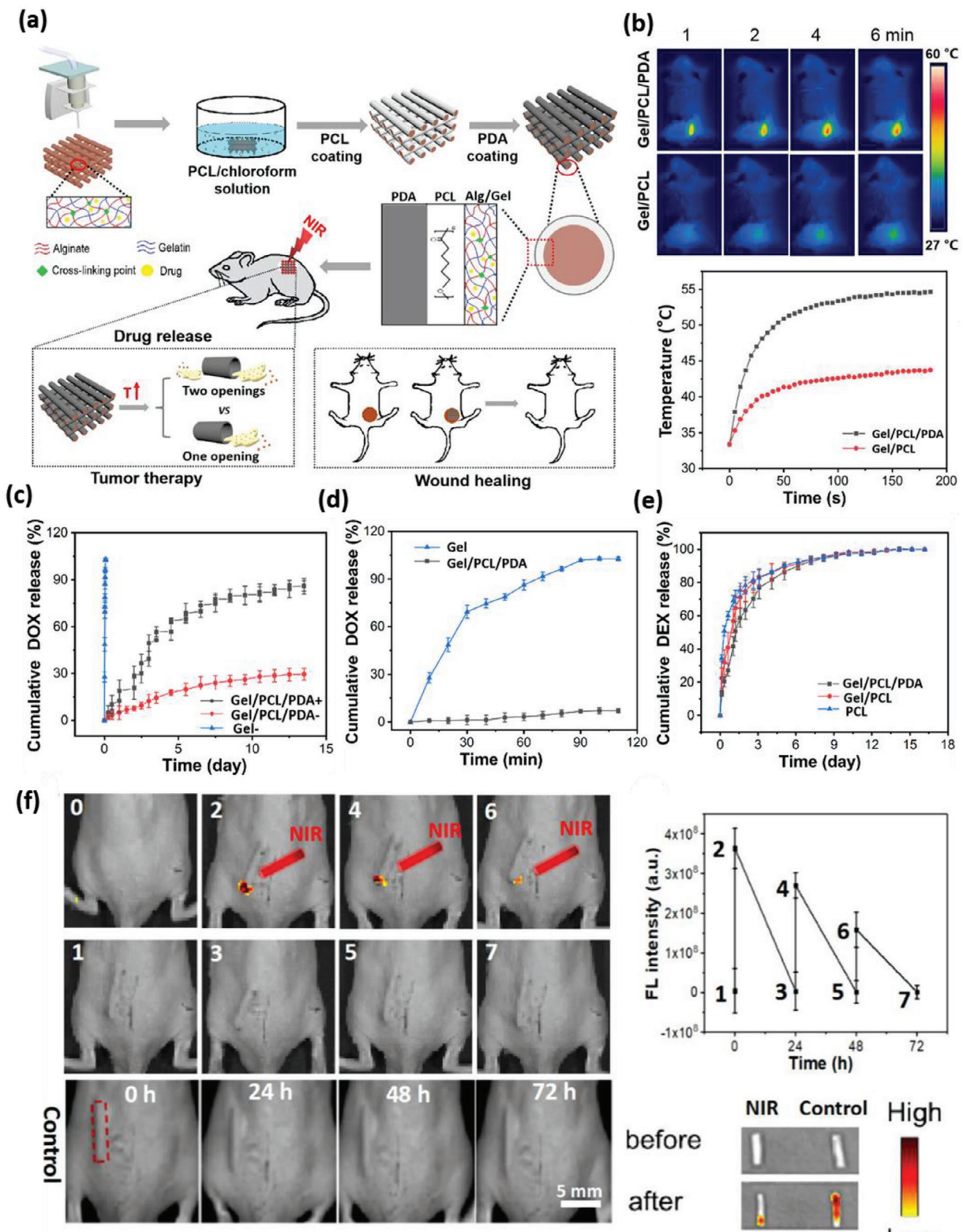


Figure 13. a) The procedure for making PDA-coated Gel/PCL core/shell scaffolds with NIR-activated on-demand medication release for tumor therapy and wound healing. b) Thermal images and heating curves of mice after the transplantation of Gel/PCL/PDA or Gel/PCL scaffolds under laser irradiation (0.5 W cm^{-2}) for 6 min. c) DOX release from alginate/gelatin (Gel) and gel/PCL/PDA scaffolds printed with repetitive laser on/off cycles for over 14 d without laser irradiation. d) Burst release of DOX from the gel scaffold printed within the first 110 min. e) Dexamethasone release from the PCL layer of a different scaffold over 14 d. f) The figure demonstrates that even after 48 h of transplantation, NIR laser irradiation still induces drug release from the open ends of the filaments. Reproduced with permission.^[124] Copyright 2021, Elsevier.

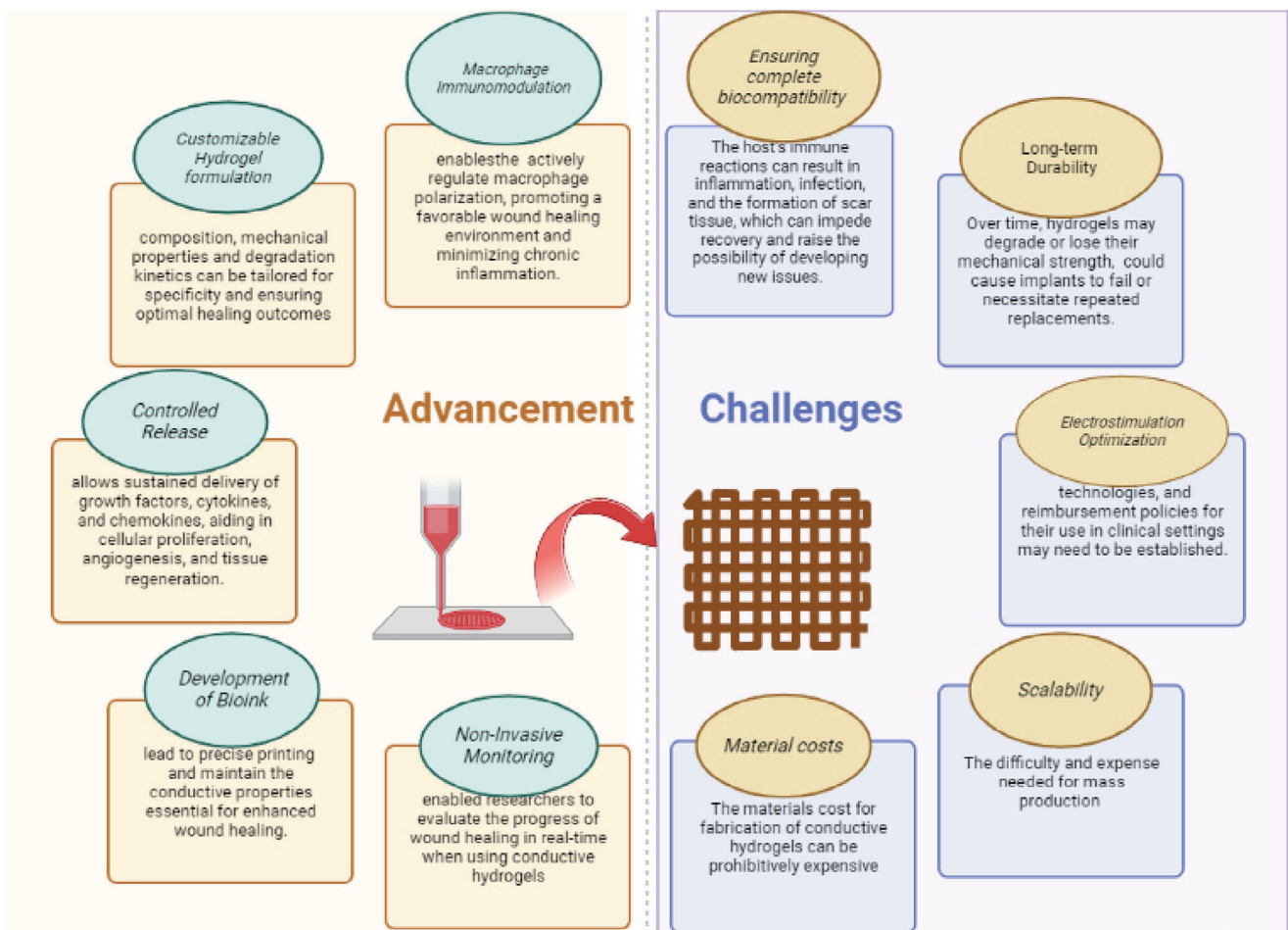


Figure 14. Schematic diagram of recent advancement and challenges of 3D printed conductive hydrogel for wound healing.

(Dex) is a nontoxic, biocompatible, and biodegradable natural polymer, making it a promising material for hydrogel-based drug delivery. The Dex-AT/HDI conductive hydrogel exhibited excellent electroactive properties and conductivity, allowing intelligent control of drug release through external electrical stimulation. In particular, the hydrogel exhibited rapid drug release under an applied voltage and minimal drug release without electrical stimuli. 3D-printed drug delivery systems have the potential to provide customized and innovative solutions based on patient needs.

Long et al. prepared hydrogels for lidocaine hydrochloride (LDC) delivery by physically crosslinking pectin (PEC) polysaccharides.^[2c] PEC is an anionic polysaccharide extracted from plant cell walls that exhibits important properties for drug delivery, such as biocompatibility and mucoadhesiveness. Chitosan and pectin are commonly crosslinked in polymer electrolyte films or networks for various drug delivery applications, including inserts, microgels, nanocarriers, bilayer patches, and controlled-release coatings. In a release study conducted in test tubes, LDC exhibited an explosive release for 1 h, followed by a sustained release for the subsequent 4 h. The porous structure of the CS-PEC hydrogel contributed to the rapid release of LDC by forming solvent uptake channels that facilitated LDC dissolution. Degradation of the CS-PEC hydrogel also contributed to fast drug

release. Because of its thermosensitive nature, a temperature increase leads to the partial breakage of hydrogen bonds between the CS and PEC chains, resulting in the partial dissolution of the CS-PEC hydrogel matrix.

7. Advances and Challenges

Inkjet printing with conductive polymers is a promising technology for wound healing and immunomodulation because of its ability to print precise patterns of electrically conductive polymers on various surfaces, including biological tissues. Conductive polymers used in inkjet printing can be designed to mimic the electrical properties of living tissues, enabling them to connect with cells and promote healing. A significant breakthrough in this area involves the application of conductive polymer hydrogels that can maintain moisture levels and create a favorable environment for cellular proliferation and wound healing. In addition, inkjet printing with conductive polymer inks allows precise control over the shape, size, and placement of the printed pattern, thereby creating customized wound dressings and tissue scaffolds. In conclusion, the development of 3D printable conductive hydrogels has emerged as a promising solution for wound healing and immunomodulation. These hydrogels

possess unique properties that enable precise fabrication, electrical stimulation, and localized delivery of bioactive molecules, contributing to enhanced wound-healing outcomes. Integrating 3D printing technology allows the creation of customized scaffolds with controlled architectures that promote cell proliferation, migration, and differentiation. The conductive nature of these hydrogels enables the application of electrical stimuli, which have demonstrated positive effects on wound-healing processes such as angiogenesis and inflammation regulation.

Moreover, conductive hydrogels can carry bioactive molecules, providing a sustained and controlled release, which is crucial for modulating immune responses during wound healing. By promoting a balanced inflammatory environment, these hydrogels contribute to optimal tissue regeneration and prevent excessive scarring. Despite significant advancements, challenges remain in optimizing the mechanical properties, biocompatibility, and degradation kinetics of hydrogels to satisfy the specific requirements of different wound types. In addition, the precise control of electrical stimulation parameters and the incorporation of suitable bioactive molecules require further research and development.

However, there are challenges associated with inkjet printing using conductive polymers, particularly in terms of biocompatibility and long-term performance. The conductive polymers used must be biocompatible, meaning that they are not toxic or harmful to living tissues, and must maintain their electrical properties over time. Furthermore, there are concerns regarding the possibility of skin irritation or allergic responses to the conductive polymers.

Comprehensive preclinical studies and regulatory considerations are essential to facilitate clinical translation of 3D printable conductive hydrogels. These studies provided a better understanding of the safety, efficacy, and long-term effects of these hydrogels *in vivo*.

In conclusion, 3D printable conductive hydrogels have great potential for revolutionizing the fields of wound healing and immunomodulation. By addressing the current limitations of traditional wound-healing strategies, these innovative hydrogels offer a pathway toward improved clinical outcomes, accelerated healing processes, and personalized approaches in wound care. Further research and collaboration between scientists, engineers, and medical professionals is crucial for overcoming the remaining challenges and unlocking the full therapeutic potential of 3D printable conductive hydrogels for wound-healing applications.

Overall, inkjet printing with conductive polymers holds great promise for transforming wound-healing and immunomodulation processes. However, additional research is required to comprehensively understand the capabilities and constraints of this technology (Figure 14).

Acknowledgements

J.L., S.D.D., and R.A. contributed equally to this work. This study was supported by the Basic Science Research Program through the National Research Foundation of Korea funded by the Ministry of Education (NRF-2018R1A1A1A03025582, NRF-2019R1D1A3A03103828, and NRF2022R111A3063302). This research was supported by the Ministry of Science and ICT, Korea, under the Innovative Human Resource Development for Local Intellectualization support program (IITP-2023-RS-2023-

00260267*) supervised by the Institute for Information and Communications Technology Planning & Evaluation.

Conflict of Interest

The authors declare no conflict of interest.

Keywords

3D printing, conductive hydrogels, electrical stimulation, immunomodulation, wound healing

Received: July 26, 2023

Revised: September 27, 2023

Published online:

- [1] V. Jones, J. E. Grey, K. G. Harding, *BMJ* **2006**, 332, 777.
- [2] a) P. Stenlund, L. Enstedt, K. M. Gilljam, S. Standoft, A. Ahlinder, M. L. Johnson, H. Lund, A. M. Fureby, M. Berglin, *Polymers* **2023**, 15, 2627; b) F. Fayyazbakhsh, M. J. Khayat, M. C. Leu, *Int. J. Bioprint.* **2022**, 8, 618; c) J. Long, A. E. Etxeberria, A. V. Nand, C. R. Bunt, S. Ray, A. Seyfoddin, *Mater. Sci. Eng., C* **2019**, 104, 109873.
- [3] D. Mohammadrezaei, N. Moghimi, S. Vandavadi, G. Powathil, S. Hamis, M. Kohandel, *Sci. Rep.* **2023**, 13, 1211.
- [4] M. J. Jang, S. K. Bae, Y. S. Jung, J. C. Kim, J. S. Kim, S. K. Park, J. S. Suh, S. J. Yi, S. H. Ahn, J. O. Lim, *Biomed. Mater.* **2021**, 16, 045013.
- [5] a) M. Milojevic, G. Harih, B. Vihar, J. Vajda, L. Gradisnik, T. Zidaric, K. S. Kleinschek, U. Maver, T. Maver, *Pharmaceutics* **2021**, 13, 564; b) J. H. Teoh, A. Mozhi, V. Sunil, S. M. Tay, J. Fuh, C.-H. Wang, *Adv. Funct. Mater.* **2021**, 31, 2105932; c) L. Yueqi, X. Jie, S. Ya, F. Huan, L. Jiaqi, L. Siyao, C. Y. Yee, N. Yi, L. Wenfang, P. Bo, *Int. J. Bioprint.* **2023**, 9, 689.
- [6] a) Z. Kong, W. Hu, F. Jiao, P. Zhang, J. Shen, Bo Cui, H. Wang, L. Liang, *J. Phys. Chem. B* **2020**, 124, 9335; b) G. Divyashri, R. V. Badhe, B. Sadanandan, V. Vijayalakshmi, M. Kumari, P. Ashrit, D. Bijukumar, M. T. Mathew, K. Shetty, A. V. Raghu, *Polym. Adv. Technol.* **2022**, 33, 2025.
- [7] a) F. Olate-Moya, L. Arens, M. Wilhelm, M. A. Mateos-Timoneda, E. Engel, H. Palza, *ACS Appl. Mater. Interfaces* **2020**, 12, 4343; b) H. Cui, Y. Yu, X. Li, Z. Sun, J. Ruan, Z. Wu, J. Qian, J. Yin, *J. Mater. Chem. B* **2019**, 7, 7207.
- [8] a) J.-J. Lee, H. Y. Ng, Y.-H. Lin, E.-W. Liu, T.-J. Lin, H.-T. Chiu, X.-R. Ho, H.-A. Yang, M.-Y. Shie, *Biomater. Adv.* **2022**, 142, 213132; b) V. Castrejón-Comas, C. Alemán, M. M. Pérez-Madrigal, *Biomater. Sci.* **2023**, 11, 2266.
- [9] D.-H. Ha, S. Chae, J. Y. Lee, J. Y. Kim, J. Yoon, T. Sen, S.-W. Lee, H. J. Kim, J. H. Cho, D.-W. Cho, *Biomaterials* **2021**, 266, 120477.
- [10] J. Barthes, P. Lagarrigue, V. Riabov, G. Lutzweiler, J. Kirsch, C. Muller, E.-J. Courtial, C. Marquette, F. Projetti, J. Kzhyksowska, P. Lavalle, N. E. Vrana, A. Dupret-Bories, *Biomaterials* **2021**, 268, 120549.
- [11] X. Wang, J. Qi, W. Zhang, Y. Pu, R. Yang, P. Wang, S. Liu, X. Tan, B. Chi, *Int. J. Biol. Macromol.* **2021**, 187, 91.
- [12] J. R. H. Sta Agueda, Q. Chen, R. D. Maalihan, J. Ren, I. G. M. Da Silva, N. P. Dugos, E. B. Caldona, R. C. Advincula, *MRS Commun.* **2021**, 11, 197.
- [13] C. Korupalli, H. Li, N. Nguyen, F.-L. Mi, Y. Chang, Y.-J. Lin, H.-W. Sung, *Adv. Healthcare Mater.* **2021**, 10, 2001384.
- [14] A. S. T. Nezakati, A. Tan, A. M. Seifalian, *Meml. Serv. Exploit. Ind. Tab. Allumettes, Ser. B* **2018**, 118, 14.
- [15] Y. Liang, L. Qiao, B. Qiao, B. Guo, *Chem. Sci.* **2023**, 14, 3091.

[16] B. Guo, Z. Ma, L. Pan, Y. Shi, *J. Polym. Sci., Part B: Polym. Phys.* **2019**, *57*, 1606.

[17] C. Yang, P. Zhang, A. Nautiyal, S. Li, N. Liu, J. Yin, K. Deng, X. Zhang, *ACS Appl. Mater. Interfaces* **2019**, *11*, 4258.

[18] D. Gan, L. Han, M. Wang, W. Xing, T. Xu, H. Zhang, K. Wang, L. Fang, X. Lu, *ACS Appl. Mater. Interfaces* **2018**, *10*, 36218.

[19] C. Wu, L. Shen, Y. Lu, C. Hu, Z. Liang, L. Long, N. Ning, J. Chen, Y. Guo, Z. Yang, *ACS Appl. Mater. Interfaces* **2021**, *13*, 52308.

[20] X. Wang, W. Zhang, Q. Zhou, F. Ran, *Chem. Eng. J.* **2023**, *452*, 139491.

[21] L. Zhao, Z. Feng, Y. Lyu, J. Yang, L. Lin, H. Bai, Y. Li, Y. Feng, Y. Chen, *Int. J. Biol. Macromol.* **2023**, *230*, 123231.

[22] X. Jing, X.-Y. Wang, H.-Y. Mi, L.-S. Turng, *Mater. Lett.* **2019**, *237*, 53.

[23] K. Chen, Y. Hu, M. Liu, F. Wang, P. Liu, Y. Yu, Q. Feng, X. Xiao, *Macromol. Mater. Eng.* **2021**, *306*, 2100341.

[24] C. Chen, Y. Wang, T. Meng, Q. Wu, L. Fang, D. Zhao, Y. Zhang, D. Li, *Cellulose* **2019**, *26*, 8843.

[25] N. Annabi, S. R. Shin, A. Tamayol, M. Miscuglio, M. A. Bakooshli, A. Assmann, P. Mostafalu, J.-Y. Sun, S. Mithieux, L. Cheung, X. (S.). Tang, A. S. Weiss, A. Khademhosseini, *Adv. Mater.* **2016**, *28*, 40.

[26] Y. Liang, X. Zhao, T. Hu, B. Chen, Z. Yin, P. X. Ma, B. Guo, *Small* **2019**, *15*, 1900046.

[27] X. Wu, H. Liao, D. Ma, M. Chao, Y. Wang, X. Jia, P. Wan, L. Zhang, *J. Mater. Chem. C* **2020**, *8*, 1788.

[28] a) A. Saberi, F. Jabbari, P. Zarrintaj, M. R. Saeb, M. Mozafari, *Biomolecules* **2019**, *9*, 448; b) L. Ghasemi-Mobarakeh, M. P. Prabhakaran, M. Morshed, M. H. Nasr-Esfahani, H. Baharvand, S. Kiani, S. S. Al-Deyab, S. Ramakrishna, *J. Tissue Eng. Regener. Med.* **2011**, *5*, e17.

[29] D. D. Ateh, H. A. Navsaria, P. Vadgama, *J. R. Soc., Interface* **2006**, *3*, 741.

[30] S. S. Athukorala, T. S. Tran, R. Balu, V. K. Truong, J. Chapman, N. K. Dutta, N. Roy Choudhury, *Polymers* **2021**, *13*, 474.

[31] K. M. Sajesh, R. Jayakumar, S. V. Nair, K. P. Chennazhi, *Int. J. Biol. Macromol.* **2013**, *62*, 465.

[32] L. Wang, S. Hu, M. W. Ullah, X. Li, Z. Shi, G. Yang, *Carbohydr. Polym.* **2020**, *249*, 116829.

[33] Y. Wang, M. Rouabdia, D. Lavertu, Z. Zhang, *J. Tissue Eng. Regener. Med.* **2017**, *11*, 110.

[34] P. Moutsatsou, K. Coopman, S. Georgiadou, *Polymers* **2017**, *9*, 687.

[35] L. Xiao, F. Hui, T. Tian, R. Yan, J. Xin, X. Zhao, Y. Jiang, Z. Zhang, Y. Kuang, N. Li, Y. Zhao, Q. Lin, *Front. Chem.* **2021**, *9*, 787886.

[36] Q. Wei, Y. Wang, L. Jia, G. Ma, X. Shi, W. Zhang, Z. Hu, *Biomater. Sci.* **2023**, *11*, 170.

[37] A. Håkansson, S. Han, S. Wang, J. Lu, S. Braun, M. Fahlman, M. Berggren, X. Crispin, S. Fabiano, *J. Polym. Sci., Part B: Polym. Phys.* **2017**, *55*, 814.

[38] L. V. Kayser, D. J. Lipomi, *Adv. Mater.* **2019**, *31*, 1806133.

[39] A. R. Spencer, E. S. Sani, J. R. Soucy, C. C. Corbet, A. Primbetova, R. A. Koppes, N. Annabi, *ACS Appl. Mater. Interfaces* **2019**, *11*, 30518.

[40] V. Vijayakumar, S. K. Samal, S. Mohanty, S. K. Nayak, *Int. J. Biol. Macromol.* **2019**, *122*, 137.

[41] a) S. W. Ali, M. Shahadat, P. Sultana, S. Z. Ahammad, *Advanced Textiles for Wound Care*, Elsevier, Amsterdam **2019**; b) J. Fong, F. Wood, *Int. J. Nanomed.* **2006**, *1*, 441.

[42] Z. B. Nqakala, N. R. S. Sibuyi, A. O. Fadaka, M. Meyer, M. O. Onani, A. M. Madiehe, *Int. J. Mol. Sci.* **2021**, *22*, 11272.

[43] J. Wu, Y. Zheng, X. Wen, Q. Lin, X. Chen, Z. Wu, *Biomed. Mater.* **2014**, *9*, 035005.

[44] R. R. Palerm, K. M. Rao, T. J. Kang, *Carbohydr. Polym.* **2019**, *223*, 115074.

[45] a) P. Pengo, M. Sologan, L. Pasquato, F. Guida, S. Pacor, A. Tossi, F. Stellacci, D. Marson, S. Boccardo, S. Pricl, P. Posocco, *Eur. Biophys. J.* **2017**, *46*, 749; b) S. Ashraf, B. Pelaz, P. del Pino, M. Carril, A. Escudero, W. J. Parak, M. G. Soliman, Q. Zhang, C. Carrillo-Carrion, *Light-Responsive Nanostructured Systems for Applications in Nanomedicine*, Springer, Cham **2016**, p. 169.

[46] S. Al-Musawi, S. Albuhaty, H. Al-Karagoly, G. M. Sulaiman, M. S. Alwahibi, Y. H. Dewir, D. A. Soliman, H. Rizwana, *Molecules* **2020**, *25*, 4770.

[47] K. M. Zepon, M. S. Marques, A. W. Hansen, C. d. A. F. Pucci, F. D. P. Morisso, A. L. Ziulkoski, J. H. O. do Nascimento, R. F. Magnago, L. A. Kanis, *Mater. Sci. Eng., C* **2020**, *109*, 110630.

[48] Z. Deng, M. Li, Y. Hu, Y. He, B. Tao, Z. Yuan, R. Wang, M. Chen, Z. Luo, K. Cai, *Chem. Eng. J.* **2021**, *420*, 129668.

[49] A. H. Hashem, A. M. Shehabeldine, O. M. Ali, S. S. Salem, *Polymers* **2022**, *14*, 2293.

[50] Q. Zhao, S. Mu, X. Liu, G. Qiu, D. Astruc, H. Gu, *Macromol. Chem. Phys.* **2019**, *220*, 1800427.

[51] G. Borkow, J. Gabbay, R. Dardik, A. I. Eidelman, Y. Lavie, Y. Grunfeld, S. Ikhier, M. Huszar, R. C. Zatcoff, M. Marikovsky, *Wound Repair Regener.* **2010**, *18*, 266.

[52] Z. Li, X. Huang, L. Lin, Y. Jiao, C. Zhou, Z. Liu, *Chem. Eng. J.* **2021**, *419*, 129488.

[53] S. Zhao, L. Li, H. Wang, Y. Zhang, X. Cheng, N. Zhou, M. N. Rahaman, Z. Liu, W. Huang, C. Zhang, *Biomaterials* **2015**, *53*, 379.

[54] S. Alizadeh, B. Seyedalipour, S. Shafeyan, A. Kheime, P. Mohammadi, N. Aghdam, *Biochem. Biophys. Res. Commun.* **2019**, *517*, 684.

[55] a) W. Feng, F. Ye, W. Xue, Z. Zhou, Y. J. Kang, *Mol. Pharmacol.* **2009**, *75*, 174; b) R. R. Renuka, A. Julius, S. T. Yoganandham, D. Umapathy, R. Ramadoss, A. V. Samrot, D. D. Vijay, *Front. Endocrinol.* **2022**, *13*, 8.

[56] S. Sen, K. Sarkar, *Microb. Drug Resist.* **2021**, *27*, 616.

[57] G. Wang, J. Ye, M. Wang, Y. Qi, S. Zhang, L. Shi, Y. Fang, Y. Tian, G. Ning, *Carbohydr. Polym.* **2022**, *291*, 119588.

[58] R. Coronado, S. Pekerar, A. T. Lorenzo, M. A. Sabino, *Polym. Bull.* **2011**, *67*, 101.

[59] B. A. Costa, M. P. Abuçayf, T. W. L. Barbosa, B. L. Da Silva, R. B. Fulindi, G. Isquibola, P. I. Da Costa, L. A. Chiavacci, *Pharmaceutics* **2023**, *15*, 259.

[60] S. V. Gudkov, D. E. Burmistrov, D. A. Serov, M. B. Rebezov, A. A. Semenova, A. B. Lisitsyn, *Front. Phys.* **2021**, *9*, 641481.

[61] Y. Xie, Y. He, P. L. Irwin, T. Jin, X. Shi, *Appl. Environ. Microbiol.* **2011**, *77*, 2325.

[62] P. Pino, F. Bosco, C. Mollea, B. Onida, *Pharmaceutics* **2023**, *15*, 970.

[63] a) N. Annabi, A. Tamayol, J. A. Uquillas, M. Akbari, L. E. Bertassoni, C. Cha, G. Camci-Unal, M. R. Dokmeci, N. A. Peppas, A. Khademhosseini, *Adv. Mater.* **2014**, *26*, 85; b) S. Iqbal, H. Khatoon, A. H. Pandit, S. Ahmad, *Mater. Sci. Energy Technol.* **2019**, *2*, 417.

[64] R. Alshehri, A. M. Ilyas, A. Hasan, A. Arnaout, F. Ahmed, A. Memic, *J. Med. Chem.* **2016**, *59*, 8149.

[65] A. Vashist, A. Kaushik, A. Vashist, V. Sagar, A. Ghosal, Y. K. Gupta, S. Ahmad, M. Nair, *Adv. Healthcare Mater.* **2018**, *7*, 1701213.

[66] T. V. Patil, D. K. Patel, S. D. Dutta, K. Ganguly, A. Randhawa, K.-T. Lim, *Appl. Sci.* **2021**, *11*, 9550.

[67] J. He, M. Shi, Y. Liang, B. Guo, *Chem. Eng. J.* **2020**, *394*, 124888.

[68] A. A. Adewunmi, S. Ismail, A. S. Sultan, *J. Inorg. Organomet. Polym. Mater.* **2016**, *26*, 717.

[69] W. S. Al-Arjan, M. U. A. Khan, H. H. Almutairi, S. M. Alharbi, S. I. A. Razak, *Polymers* **2022**, *14*, 1949.

[70] C. Chen, Y. Xi, Y. Weng, *Materials* **2022**, *15*, 2164.

[71] Q. Zhong, Y. Li, G. Zhang, *Chem. Eng. J.* **2021**, *409*, 128099.

[72] K. Wang, J. Li, G. Zhang, *ACS Appl. Mater. Interfaces* **2019**, *11*, 27686.

[73] X. Zhan, C. Si, J. Zhou, Z. Sun, *Nanoscale Horiz.* **2020**, *5*, 235.

[74] Y.-Z. Zhang, J. K. El-Demellawi, Q. Jiang, G. Ge, H. Liang, K. Lee, X. Dong, H. N. Alshareef, *Chem. Soc. Rev.* **2020**, *49*, 7229.

[75] J. Zhang, L. Wan, Y. Gao, X. Fang, T. Lu, L. Pan, F. Xuan, *Adv. Electron. Mater.* **2019**, *5*, 1900285.

[76] G. Ge, Y.-Z. Zhang, W. Zhang, W. Yuan, J. K. El-Demellawi, P. Zhang, E. Di Fabrizio, X. Dong, H. N. Alshareef, *ACS Nano* **2021**, *15*, 2698.

[77] X. Zhao, H. Wu, B. Guo, R. Dong, Y. Qiu, P. X. Ma, *Biomaterials* **2017**, *122*, 34.

[78] R. Luo, J. Dai, J. Zhang, Z. Li, *Adv. Healthcare Mater.* **2021**, *10*, 2100557.

[79] E. Fantino, I. Roppolo, D. Zhang, J. Xiao, A. Chiappone, M. Castellino, Q. Guo, C. F. Pirri, J. Yang, *Macromol. Mater. Eng.* **2018**, *303*, 1700356.

[80] G. Ge, Q. Wang, Y.-Z. Zhang, H. N. Alshareef, X. Dong, *Adv. Funct. Mater.* **2021**, *31*, 2107437.

[81] T. Distler, A. R. Boccaccini, *Acta Biomater.* **2020**, *101*, 1.

[82] H. Quan, T. Zhang, H. Xu, S. Luo, J. Nie, X. Zhu, *Bioact. Mater.* **2020**, *5*, 110.

[83] D. N. Heo, S.-J. Lee, R. Timsina, X. Qiu, N. J. Castro, L. G. Zhang, *Mater. Sci. Eng., C* **2019**, *99*, 582.

[84] S. H. Kim, D. Y. Kim, T. H. Lim, C. H. Park, *Bioinspired Biomaterials: Advances in Tissue Engineering and Regenerative Medicine*, Springer, Singapore **2020**, p. 53.

[85] A. Jennifer, S. Manivannan, S. Sethuraman, S. G. Kumbar, D. Sundaramurthi, *Biomater. Adv.* **2022**, *134*, 112576.

[86] a) M. Müller, J. Becher, M. Schnabelrauch, M. Zenobi-Wong, *Biofabrication* **2015**, *7*, 035006; b) K. S. Lim, R. Levato, P. F. Costa, M. D. Castilho, C. R. Alcalá-Orozco, K. M. A. Van Dorenmalen, F. P. W. Melchels, D. Gawlikka, G. J. Hooper, J. Malda, T. B. F. Woodfield, *Biofabrication* **2018**, *10*, 034101; c) B. Grigoryan, S. J. Paulsen, D. C. Corbett, D. W. Sazer, C. L. Fortin, A. J. Zaita, P. T. Greenfield, N. J. Calafat, J. P. Gounley, A. H. Ta, F. Johansson, A. Randles, J. E. Rosenkrantz, J. D. Louis-Rosenberg, P. A. Galie, K. R. Stevens, J. S. Miller, *Science* **2019**, *364*, 458; d) D. E. Mccoy, T. Feo, T. A. Harvey, R. O. Prum, *Nat. Commun.* **2018**, *9*, 1.

[87] L. Wang, Q. Wang, A. Slita, O. Backman, Z. Gounani, E. Rosqvist, J. Peltonen, S. Willför, C. Xu, J. M. Rosenholm, X. Wang, *Green Chem.* **2022**, *24*, 2129.

[88] Y. Guo, H. S. Patanwala, B. Bognet, A. W. K. Ma, *Rapid Prototyping J.* **2017**, *23*, 562.

[89] G. Cummins, M. P. Y. Desmulliez, *Circuit World* **2012**, *38*, 193.

[90] S. Kawale, I. Jang, N. Farandos, G. Kelsall, *React. Chem. Eng.* **2022**, *7*, 1692.

[91] D. Zhao, H. Zhou, Y. Wang, J. Yin, Y. Huang, *Addit. Manuf.* **2021**, *48*, 102451.

[92] J. Bush, C.-H. Hu, R. Veneziano, *Appl. Sci.* **2021**, *11*, 1885.

[93] M. Chountoulesi, D. Selianitis, S. Pispas, N. Pippa, *Materials* **2023**, *16*, 2298.

[94] G. Yang, Y. Sun, L. Qin, M. Li, K. Ou, J. Fang, Q. Fu, *Compos. Sci. Technol.* **2021**, *215*, 109013.

[95] M. A. S. R. Saadi, A. Maguire, N. T. Pottackal, Md. S. H. Thakur, M. Md. Ikram, A. J. Hart, P. M. Ajayan, M. M. Rahman, *Adv. Mater.* **2022**, *34*, 2108855.

[96] J. Liu, L. Sun, W. Xu, Q. Wang, S. Yu, J. Sun, *Carbohydr. Polym.* **2019**, *207*, 297.

[97] M. Mao, J. He, X. Li, B. Zhang, Q. Lei, Y. Liu, D. Li, *Micromachines* **2017**, *8*, 113.

[98] J. Liu, J. Garcia, L. M. Leahy, R. Song, D. Mullarkey, B. Fei, A. Dervan, I. V. Shvets, P. Stamenov, W. Wang, F. J. O'brien, J. N. Coleman, V. Nicolosi, *Adv. Funct. Mater.* **2023**, *33*, 2214196.

[99] W. Sun, A. Feinberg, V. Webster-Wood, *HardwareX* **2022**, *11*, e00297.

[100] J. Liu, L. Yang, K. Liu, F. Gao, *Front. Pharmacol.* **2023**, *14*, 1050954.

[101] Z. Wang, Y. Sun, W. Yao, Q. Ba, H. Wang, *Front. Immunol.* **2021**, *12*, 695484.

[102] Z. Tong, L. Jin, J. M. Oliveira, R. L. Reis, Q. Zhong, Z. Mao, C. Gao, *Bioact. Mater.* **2021**, *6*, 1375.

[103] C. Chen, T. Liu, Y. Tang, G. Luo, G. Liang, W. He, *Int. J. Burns Trauma* **2023**, *11*, 57.

[104] a) B. Tiller, A. Reid, B. Zhu, J. Guerreiro, R. Domingo-Roca, J. C. Jackson, J. Windmill, *Mater. Des.* **2019**, *165*, 107593; b) L. Ge, L. Dong, D. Wang, Q. Ge, G. Gu, *Sens. Actuators, A* **2018**, *273*, 285; c) M. Sharafeldin, A. Jones, J. Rusling, *Micromachines* **2018**, *9*, 394.

[105] a) M. S. Mannoor, Z. Jiang, T. James, Y. L. Kong, K. A. Malatesta, W. O. Soboyejo, N. Verma, D. H. Gracias, M. C. Mcalpine, *Nano Lett.* **2013**, *13*, 2634; b) Z.-X. Low, Y. T. Chua, B. M. Ray, D. Mattia, I. S. Metcalfe, D. A. Patterson, *J. Membr. Sci.* **2017**, *523*, 596.

[106] J. X. Zhang, K. Hoshino, *Molecular Sensors and Nanodevices: Principles, Designs and Applications in Biomedical Engineering*, Academic, San Diego, CA **2018**.

[107] a) J. F. Rusling, *ACS Sens.* **2018**, *3*, 522; b) K. Wang, C.-C. Ho, C. Zhang, B. Wang, *Engineering* **2017**, *3*, 653.

[108] a) T. M. Valentini, S. E. Leggett, P.-Y. Chen, J. K. Sodhi, L. H. Stephens, H. D. Mcclintock, J. Y. Sim, I. Y. Wong, *Lab Chip* **2017**, *17*, 3474; b) S. S. Hirman, K. S. McKeating, Q. Cheng, *Anal. Chem.* **2017**, *89*, 12626; c) Z. Wang, H. Kumar, Z. Tian, X. Jin, J. F. Holzman, F. Menard, K. Kim, *ACS Appl. Mater. Interfaces* **2018**, *10*, 26859.

[109] a) B. J. Rumley-Ouellette, J. H. Wahry, A. M. Baker, J. D. Bernardin, A. N. Marchi, M. D. Todd, *Struct. Health Monit.* **2017**, <https://doi.org/10.12783/shm2017/14071>; b) L. Cevenini, M. M. Calabretta, G. Tarantino, E. Michelini, A. Roda, *Sens. Actuators, B* **2016**, *225*, 249; c) D. Pranzo, P. Larizza, D. Filippini, G. Percoco, *Micromachines* **2018**, *9*, 374; d) A. H. Loo, C. K. Chua, M. Pumera, *Analyst* **2017**, *142*, 279; e) Y. Song, S. Nesaei, D. Du, A. Gozen, Y. Lin, *Electrochemical Society Meeting Abstracts* **233**, *2018*; f) J. L. Connell, J. Kim, J. B. Shear, A. J. Bard, M. Whiteley, *Proc. Natl. Acad. Sci. USA* **2014**, *111*, 18255.

[110] F. Tsegay, M. Elsherif, H. Butt, *Polymers* **2022**, *14*, 1012.

[111] G. Torkaman, *Adv. Wound Care* **2014**, *3*, 202.

[112] H. Lei, D. Fan, *Chem. Eng. J.* **2021**, *421*, 129578.

[113] X. Ding, Y. Yu, C. Yang, D. Wu, Y. Zhao, *Research* **2022**, *2022*, 14.

[114] a) J. Tan, Q.-Y. Zhang, Y.-T. Song, K. Huang, Y.-L. Jiang, J. Chen, R. Wang, C.-Y. Zou, Q.-J. Li, B.-Q. Qin, N. Sheng, R. Nie, Z.-Y. Feng, D.-Z. Yang, W.-H. Yi, H.-Q. Xie, *Composites, Part B* **2022**, *243*, 110149; b) M. M. Alvarez, J. C. Liu, G. Trujillo-De Santiago, B.-H. Cha, A. Vishwakarma, A. M. Ghaemmaghami, A. Khademhosseini, *J. Controlled Release* **2016**, *240*, 349.

[115] S. D. Dutta, K. Ganguly, J. Hexiu, A. Randhawa, Md Moniruzzaman, K.-T. Lim, *Macromol. Biosci.* **2023**, *23*, 2300096.

[116] Z. Julier, A. J. Park, P. S. Briquez, M. M. Martino, *Acta Biomater.* **2017**, *53*, 13.

[117] W. Cao, S. Peng, Y. Yao, J. Xie, S. Li, C. Tu, C. Gao, *Acta Biomater.* **2022**, *152*, 60.

[118] a) S. Kennedy, C. Roco, A. Délérés, P. Spoerri, C. Cezar, J. Weaver, H. Vandeburgh, D. Mooney, *Biomaterials* **2018**, *161*, 179; b) X. Wei, C. Liu, Z. Wang, Y. Luo, *Int. J. Pharm.* **2020**, *580*, 119219.

[119] F. Lin, J. Zheng, W. Guo, Z. Zhu, Z. Wang, B. Dong, C. Lin, B. Huang, B. Lu, *Cellulose* **2019**, *26*, 6861.

[120] P. Sun, T. Huang, X. Wang, G. Wang, Z. Liu, G. Chen, Q. Fan, *Biomacromolecules* **2019**, *21*, 556.

[121] D. Huang, M. Sun, Y. Bu, F. Luo, C. Lin, Z. Lin, Z. Weng, F. Yang, D. Wu, *J. Mater. Chem. B* **2019**, *7*, 2330.

[122] H. Ding, B. Li, Y. Jiang, G. Liu, S. Pu, Y. Feng, D. Jia, Y. Zhou, *Carbohydr. Polym.* **2021**, *251*, 117101.

[123] H.-W. Liu, S.-H. Hu, Y.-W. Chen, S.-Y. Chen, *J. Mater. Chem.* **2012**, *22*, 17311.

[124] C. Liu, Z. Wang, X. Wei, B. Chen, Y. Luo, *Acta Biomater.* **2021**, *131*, 314.

[125] E. Vorndran, U. Klammt, A. Ewald, J. E. Barralet, U. Gbureck, *Adv. Funct. Mater.* **2010**, *20*, 1585.

[126] J. Qu, Y. Liang, M. Shi, B. Guo, Y. Gao, Z. Yin, *Int. J. Biol. Macromol.* **2019**, *140*, 255.



Jieun Lee is a master's student in biosystems engineering at Kangwon National University, South Korea. Her research is the development of various conductive 3D hydrogels for tissue regeneration and healing.



Sayan Deb Dutta is a postdoctoral research associate at Kangwon National University. He received his doctoral degree from the Department of Biosystems Engineering at Kangwon National University, South Korea. He reviewed his master's degree from the University of Kalyani, India. His research interest is the synthesis of multifunctional nanomaterials for 3D printing and nanotheranostic applications for tissue engineering.



Rumi Acharya is a doctoral student in biosystems engineering at Kangwon National University, South Korea. She received her master's degree from Guru Ghasidas University, India. Her research interests are nano biosensors and magnetogenetic therapy on cellular targets.



Hyeonseo Park is a master's student in biosystems engineering at Kangwon National University, South Korea. Her research interest is guided wound healing using nanofiber scaffolds through an electrospinning technique.



Hojin Kim is a master's student in biosystems engineering at Kangwon National University, South Korea. His research interest is nanocellulose hydrogel for wound healing and sensing.



Ayushi Randhawa is a doctoral student in biosystems engineering at Kangwon National University, South Korea. She received her master's degree from Bangalore University, India. Her research interest is the synthesis of 3D-printed structures for the healing and regeneration of damaged bone tissues.



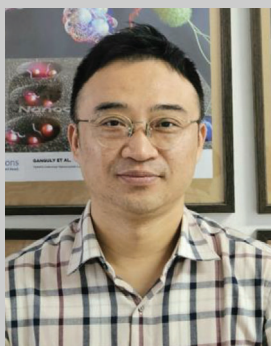
Tejal V. Patil is a doctoral student of biosystems engineering at Kangwon National University, South Korea. She received her master's degree from the Institute of Chemical Technology, Mumbai, India. Her research interest is developing biomaterials for application in bacteria eradication and tissue regeneration.



Keya Ganguly is a postdoctoral research associate at Kangwon National University. She received her doctoral degree from the Department of Biosystems Engineering at Kangwon National University, South Korea. She received her master's degree from Presidency University, India. Her research interest is developing a multistimuli-assisted scaffolding platform for tissue engineering and biosensing.



Rachmi Luthfikasari received her master's degree from the Department of Biosystems Engineering at Kangwon National University, South Korea. She received her bachelor's degree in biology from the University of Indonesia, Indonesia. Her research interest is biomimetic material and its application in tissue engineering.



Ki-Taek Lim is a professor at the Department of Biosystems Engineering at Kangwon National University, South Korea. He received his doctoral degree from Seoul National University, South Korea, and joined as a postdoctoral research fellow at the University of Arkansas, USA. He has a strong knowledge of mechatronics and regenerative medicines. His research focuses on developing the bio-nanorobotics system with novel bioreactors and stem cell cultures for tissue-engineering applications.